General Doping Chemistry of Carbon Materials

Mohammad Boshir Ahmed[a,b,d, e#*], Jahangir Alom[b#], Md. Saif Hasan[b#], Md. Asaduzaman[b#], Saifur Rahman[c], Rakibul Hasan[a], MAH Johir[d], Mohammad Taufiq Alam[b], John L Zhou[d], Masoumeh Zargar[e].

[a]School of Material Science and Engineering, Gwangju Institute of Science and Technology, Gwangju 61005, Republic of Korea

[b]Department of Applied Chemistry and Chemical Engineering, University of Rajshahi, Rajshahi 6205, Bangladesh

[c]Department of Biomedical Engineering, Texas A&M University, College Station, TX, United States

[d]Center for Green Technologies, School of Civil and Environmental Engineering, University of Technology Sydney, 15, Broadway, Sydney, NSW 2007, Australia

[e]School of Engineering, Edith Cowan University, Joondalup, WA 6027, Australia.

[#] = ***Equally contributed.***

Abstract

Carbon has an exceptional capacity to bind with itself and other elements, giving unique structures and allowing for various applications. Recently, intensive research is has been focused on the properties of carbon-based materials (CBMs) and on increasing their performance by doping with metals and non-metallic elements. While materials with excellent performance have been experimentally achieved, a fundamental knowledge of the relationship between the electronic, physical, and electrochemical properties and their structural features, particularly the chemistry of the carbon-based materials remains a top challenge. This review will start from the doping chemistries of CBMs, to cover the the role of electron affinity; reaction free energy; orbital chemistry; the chemistry of band gap, conductivity; bonding type; spin redistribution, and to conduct relevant comparisons, to provide an in-depth understanding of the overall picture in the CBMs. The future research prospects and challenges for doped CBMs will also be highlighted.

1. Introduction

Carbon element has an extraordinary ability to combine with itself and other elements in various ways to form millions of compounds which is the basis of modern organic and composite chemistry. Carbon has long been used for different applications with its three different allotropes. For example, carbon can be in (i) crystalline forms such as cubic diamond, graphite, hexagonal graphite, fullerenes and carbynes; (ii) amorphous carbons such as carbon fiber, activated carbon, char, biochar, micro-and mesoporous carbon, carbon films and diamond films; and (iii) carbon nanoparticles including graphitic carbon, carbon nanotubes (CNTs), and nanocarbons. Therefore, each allotrope has different properties based on its atomic arrangements[1]. For example, carbon allotrope graphite is very soft, black, and very stable in strong acid and basic media. On the contrary, diamond is the hardest engineering material of carbon ever known and is highly transparent. However, the subsequent discovery of graphene and CNTs opened up a new era in carbon elemental chemistry, which is gaining considerable attention in recent years as one of the most active research fields. Due to the unique structures of different carbon materials, they are found to be very interesting in different fields in catalysts, electronic devices including flexible electronics, photonics, solar cells, energy conversion and storage, environmental applications, magnetic, electric, and electrocatalytic applications, and so on[2,3].

Doping is the intentional introduction of impurities into a material to modify its parent properties[4]. It is a fundamental mechanism in controlling the properties of pristine carbon-based materials (CBMs). Over the last few decades, a significant increase has been documented in doping chemistry, from fundamental chemistry to complex synthesis, leading to different materials. **Fig. 1** shows the recent progresses of carbon doping research and effects of dopant concentration on the properties. From the graph it can be seen that CBMs such as graphene, CNTs, mesoporous and microporous carbon, nanocarbon, activated carbon, and biochar and so on have been extensively doped to achieve new functionalities. Among them graphene and graphene oxides are mostly reported for the preparation of different composites with different dopant concentration, and have achieved properties close to idealized values, but still their remain a gap between the theoretical dopant concentration and those found in experimental values.

Those carbon-based materials are extremely promising alternatives to the all metal or metal oxide-based catalysts, due to their many advantages, such as CBMs are essentially low-cost, structural flexibility beyond atomic scale, excellent electronic conductivity, high specific surface area, and good stability in a wide range of acid and basic media. Moreover, their electronic structure is tunable via different types of doping, making them attractive in different applications such as low-dimensional organic electronics, photovoltaics, catalysis, solar cells, and alike. Therefore, doping of CBMs has become a common stretagy nowadays. As a result, in recent years, tremendous efforts have been put forward to the investigation of new types of dopant to improve the performance of the CBMs over pristine CBMs for different applications. As a part of this chemical doping, chemical vapor deposition, UV radiation, microwave treatment, metal and nonmetal contact doping, electrochemical doping, solution-based processes, and other methods have been successfully used for changing the electronic structure and morphology of CBMs through doping[5]. Therefore, when a carbon material is doped with a dopant, charged sites will be created on the carbon support, which could act as strong active sites for electrochemical reactions (i.e., can work as a catalyst). This will change the electronic structure of each other, thereby increasing its activity as a catalyst[6-9].

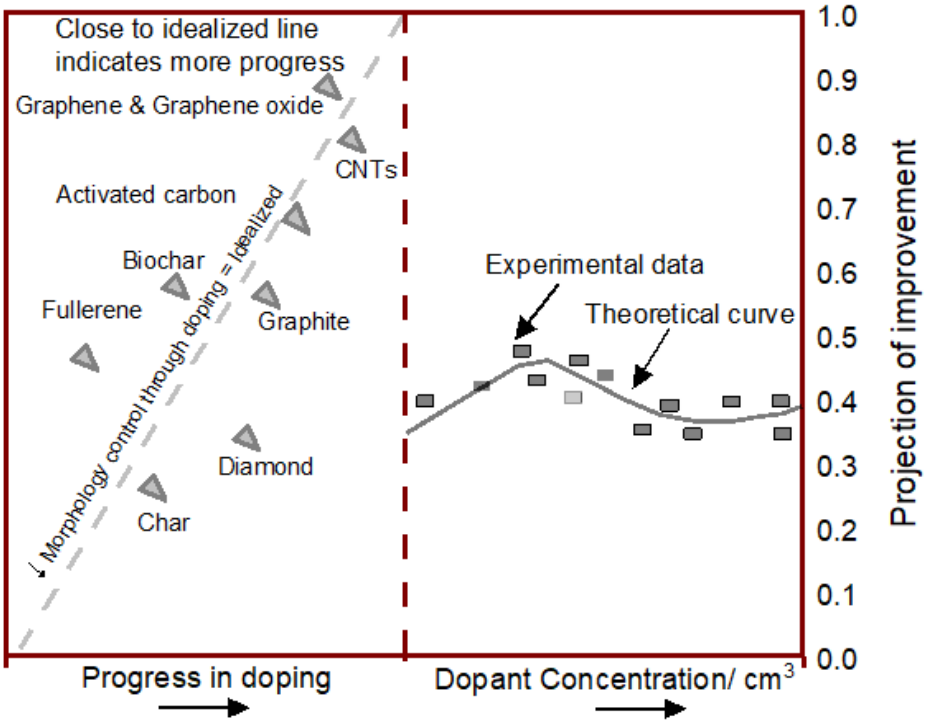

Fig. 1: Recent progress of CBMs doping and effect of dopant concentration based on experimental and theoretical concepts.

There are some studies already available on carbon materials doping. They are mainly based on particular element/s doping. For example, recently, Inagaki et al.,[10] reviewed on the nitrogen-doped carbon materials. Similarly, Deng et at.,[11] studied on the recent advances in nitrogen-doping carbons. Also, Agnoli and Favoro[12] studied on graphene doping with borod. Similar kinds of other studies are also available. Although extensive focus has been made on the chemical doping of CBMs, the underlying mechanism and chemistry of doping has yet to be fully understood. The main problem arises from the complex electronic structure of CBMs and dopants[13]. Further complexity is observed for bi-tri or more hetero atom doping in CBMs. Therefore, this review focused on the fundamental chemistry of CBMs doping, with special emphasis given to the underlying mechanism of doping of CBMs based on both the dopant and CMBs properties.

2. Principle Chemistries Based on Orientation of the Elements in CBMs

Doping is the process of controlling the properties of the materials. CBMs can be doped based on dopant properties. For example, a dopant can be either an electron donor or an electron acceptor. In the core structure of carbon networks in CMBs, the dopant (i.e., single atom or heteroatoms or compound or both) must not be positioned in a way that is exclusively substitutional to significantly affect the original structures. This is because the position of each atom at the C-network can significantly influence the properties of the materials. For example, if carbon is doped with an N atom in the graphitic lattice by direct substituting C atoms, which contains an additional electron pair compared to carbon's socalled n-type doping material then novel electronic properties are expected[14]. In addition, due to different sizes of the dopant and host (C-network), n-type dopant, i.e., N can generate a defect in the core structure of the C-network and thus require atomic rearrangement of the C atoms; thereby, a new geometry will be generated which will lead to a different wall structures. Moreover, some atoms can be also encapsulated in the core of the C-network or trapped within the bundles of intercalated shells. Furthermore, the

elimination of C atoms from the C-network can induce defect structures based on the type of doping methods. Thus, the electronic properties are greatly changed from the pristine C-network[15]. Similarly, an opposite case may happen for p-type doping, i.e., when an electron pair vacant atom (e.g., B atom in C-network) is incorporated into the core structure of the C-network. As a result of doping, the host CMBs are intercalated with dopants in the inter-shell spaces or their core structure or can form outer shell intercalation. This kind of dopant intercalation to CBMs unit can be carried out in the liquid phase, vapor phase or both, and electrochemically or in other methods[14]. However, the main considerations of doping include Fermi-level-induced compensation effects, chemical potentials of the different elements, and local bonding effects of the dopant to the lattice[16]. The following equation shows the combination of these effects.

$$\Delta H^{(D,q)}(\mu, E_F) = qE_F + n_D(\mu_D - \mu_H) + \Delta E_b \qquad (1)$$

where H is the formation enthalpy of dopant D, q is the charge state of dopant in the host, μ_D is the dopant chemical potential of the dopant, μ_H is the chemical potential of the host, E_F is the electro-chemical potential (Fermi energy), n_D is the number of dopants, $\Delta E_b = E$ (host + defect)-E(host) is the excess energy of the local chemical bonds around the dopant, and E is the total energy[16]**. Fig. 2** illustrates the basic principle of carbon doping (**2a**); different elements orientation in CBMs (**2b**) and ternary diagram of carbon doping with B and N elements (**2c**).

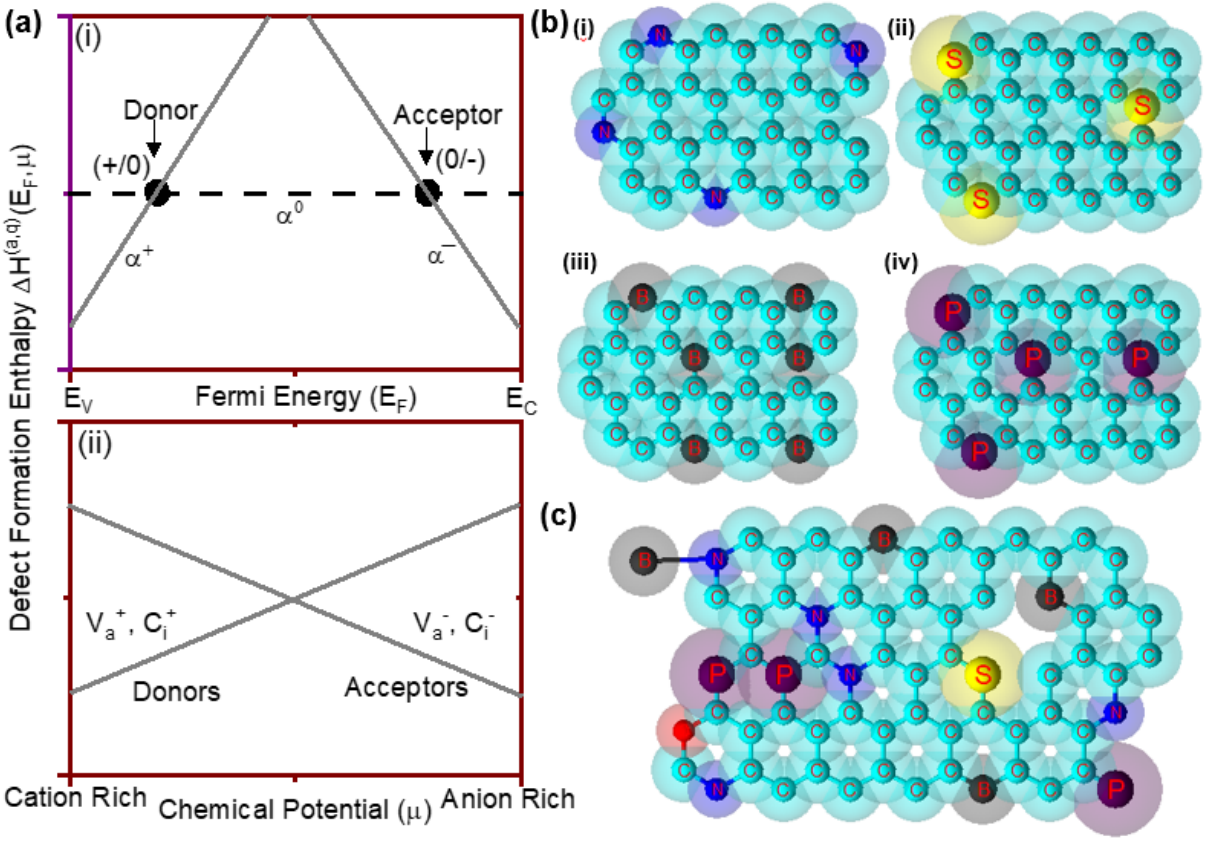

Fig. 2: (a) Principle of doping chemistry, (b) Orientation of different elements in CBMs, and (c) Ternary diagram for C, B and N doping of CBMs.

At the zero charge state of the dopant, no electron transfers happen (**Fig. 2a**). But, when a dopant which produces an electron acting as an electron donor α (i.e., the charge of dopant $q>0$) is incorporated into a host whose energy is E_F, then it denotes electrons. Therefore, the total donor formation energy increases linearly with E_F (equation 1). On the other hand, electron withdrawing acceptors (i.e., $q<0$) entail removing q electrons from the Fermi reservoir. Therefore, the electron acceptor formation energy will decrease linearly with E_F [16]. When we intentionally dope materials with a donor (i.e., n-type), the formation energy shifts towards the conduction band (**Fig. 2a**). This will ultimately lead to a spontaneous decrease of the acceptor formation energy by cation vacancies. Therefore, doping of a material (n-type via donors) needs

to shift E_F towards the conduction band and the formation energy of nearby electron acceptors will decrease to a position from where the spontaneous electron happens[16].

2.1. Mono Heteroatom Doping of CBMs

Insertion of different atoms (e.g., N, B, O, S, X, M, and so on) in CBMs has been mainly carried out for electrical modulation to tune their physicochemical and electronic properties as well as chemical activities for boosting their applications in different fields[17]. Doping of CBMs with heteroatoms is gaining popularity nowadays for tuning the surface properties to boost the catalytic activity of CBMs. These kinds of insertion can mainly be carried out by in-situ doping during the CBMs synthesis stage or through post-chemical or physical treatments with those atoms-containing precursors. The general idea is that in-situ doping of CBMs is very good for obtaining homogenous structures with doped elements. In contrast, post-doping of CBMs leads to a change in the surface functionalization without altering the bulk CBMs properties[2,18-20]. **Fig. 2b** provides possible illustrations for changes in the C-structure induced by different dopants (if would place separately so called monodoping). Many non-metal and metal elements are shown in the C-core structure. However, the electron density of pristine graphene is uniform, where most of the electrons placed between the C-C bond with little amount of center electron in the hexagon, resulting in the π electrons being inert that cannot contribute to the catalytic performance. So, it is obvious that the insertion of dopant in C-structure causes an electron modulation to change the charge distribution and electronic properties. Therefore, these kinds of changes by doping-induced defects can also change the chemical activity and reactivity of CMBs, which will lead to many applications[21-23]. For instance, doped N atom in graphene influences their electron distribution by attracting electrons due to the greater electronegativity or electron-withdrawing nature and forms a high electron area [24].

According to the principle of doping, dopant leads to a compassionate change in the Fermi level toward a conduction band even in the presence of mono atom in parts per million levels. Therefore, the substitute of carbon atoms with heteroatoms is highly possible to control the electronic properties of CBMs by following well defined controlled synthesis process of p- and n-doping (**Fig. 2a**)[20,25-27]. For example, Sun et al.,[20] constructed finite cluster models of

CNTs by doping with electron donor N atom (dopant concentration ~7%). In that study, the central C atom was removed to create a vacancy among hexagon CNTs, and then three C atoms around it were replaced by N atoms. This produced pyrrole N-doped CNT with a distorted structure. Hence, the concentrated N atoms were responsible for the CNT roughness. They also mentioned that N atoms with lone pair electrons bring a negative charge onto the CNTs[15,20].

On the other hand, electron-deficient element such as boron doping of CBMs has gained much attention for changing mechanical and electronic properties[28]. Change of electronic properties of CBMs is highly possible even in the presence of small concentrations of boron atoms[29-31]. The basic principle is that the B element has one pair of electron–deficient, which can uptake electrons from C atoms and combine with different proportions by introducing a new electronic state within the forbidden band, and the Fermi level shifts downward into the conduction band of the undoped CBMs[32]. In addition, doped B atoms in graphene influence their electron distribution by losses electrons due to the low electronegativity or electron donating nature, and form a low electron area [24]. Moreover, instead of C atoms substitution from CBMs, impurities in those materials can also be implemented by incorporating or intercalating foreign atoms into their open spaces in the carbon mash[33]. Finally, by controlling the dopant concentration, the specific conditions and doping processes, it is highly possible to achieve desired doped CBMs for many applications.

2.2. Co- Hetero Atom Doping of CBMs

Co-doping is the method of doping a material with two or more different dopants in order to increase active specific sites and regulate the work function of the host material. Moreover, heteroatom co-doping could not only enhance the surface area, the redox activity, conductivity, introduction of defects by tuning the enter layer distance and improving the porosity in carbon , but also could promote the stability of the doped CBMs. This kind of doping is mainly carried out by replacing carbon lattice atoms with certain dopants based on the dopants and host carbon affinity, electronegativity, geometry, charge density, and spin density[18,34]. Therefore, CBMs are the ideal candidates to serve this purpose. Since different dopants have different atomic sizes, dopants in carbon clouds bring a spatial distortion of the geometry, which can significantly

influence the catalytic activity of CBMs. DFT calculations have shown that the introduction of hetero dopant in carbon lattice can act as a perfect active site for adsorbing oxygen and hydrogen molecules. As described earlier, N can act as an electron donor, and B can act as an electron acceptor for carbon nanomaterials; therefore, doping with such a combination, i.e., donor-acceptor in the same SP^2 carbon lattice, can significantly increase the catalytic activity. Different combinations such as N-P-S, N-S-F, N-B-F, N-P-F, and N-P-B have been reported as active catalysts[35-41]. Hence, different co-dopant combinations such as N, B, S, P, F, Cl, and metal atom have been reported. Such a mixed example is shown in **Fig. 2c**.

Theoretically, different co-dopants can couple with the main carbon chain, which can promote charge transfer efficiency and introduce asymmetric spin density. The results showed that such kinds of configurations could easily polarize carbon atoms either by electron withdrawing (by N atom) or electron donating by carbon to dopant (such as B). This type of combination can also increase the electron occupancy to act as adsorption sites for higher catalytic activity relative to that unitary doped CBMs. For an instance, due to the redistribution of electrons, more active sites are formed around the co-doped N and B atoms in graphene when they are separated resulting in much better catalytical activity than single atom doped case[24]. However, if N and B atoms are co-doped at bonded sites, lone-pair electrons from the N atom are neutralized by the unoccupied orbital of the B atoms, leading to a high electron density between the N-B bond and low conjugation with π-electrons and bad catalytic performance[24].

On the other hand, doping with S cannot change the density significantly, as the C and S atoms have almost similar electronegativity. However, based on the practical and theoretical analyses, it has been demonstrated that S in C lattice can increase the spin density of C, which is responsible for the activity of C to be acted as a catalyst[34]. Moreover, based on the theoretical analysis, it has been found that the density state of N and S co-doped graphene and CNTs were close to its Fermi level, which showed the best catalytic activity for hydrogen evaluation reaction (HER), ORR and OER reactions under hard condition. Whereas many N-doped, N and B co-doped and N, P co-doped graphene featured the lowest Fermi level energy compared with that of the N and S co-doped graphene[42,43], a few studies have also reported on P-doped CBMs together with N-doping, which can boost the catalytic activity of CBMs[44]. This happens due to the reduction of the free energy barrier for HER, as found by DFT calculations. Moreover, this co-

doped carbon material showed higher activity for the initial H* adsorption in specific sites, such as pyridinic N- and P-doped carbon material in both strong acid and basic media[18,45].

Although heteroatom co-doping has a number of benefits and has undergone active development recently, it is still challenging in laboratory to control the amount of dopant in co-heteroatom doping and maintain a specific ration of two atoms in carbon material. In order to produce co-doped carbon with the necessary qualities, these problems will eventually need to be solved and the difficulties overcome in theoretical and experimental research.

2.3. Single Metal Atom Doping of CBMs

Metal and its compounds are used for a long time as a catalyst in different forms with varying degrees of performance. The general idea is that exposing more surfaces of these materials will lead to better activity and reactivity as catalysis. Traditional heterogeneous metal or metal compound catalysts have a broad range distributions in size, and only a small fraction of them is involved in the reaction as an active site to trigger its performance[46]. Therefore, those catalysts often suffer from low reactivity, poor stability, bad recyclability, low efficiency, high metal consumption, low surface exposure ability with cumbersome, which increased the overall cost for subsequent product purification and waste disposal[46,47]. Thereafter, much attention was put forward to minimizing the size of the particles and engineering the control of the surface morphology, in order to achieve the desired catalysts with high surface sites, high reactivity, low level of agglomeration, high efficiency, and low consumption[48-51]. **Fig. 3a** represents the changes of surface free energy and specific activity of metal supported materials with different size effects. As a part of those approaches, nanomaterials of various sizes (e.g., CNTs, graphene, nano-metal atoms, nano-inorganics and nano-organics, and alike) have been prepared through different procedures to achieve high efficiency and higher selectivity for many applications. For example, single atom catalyst (SAC) i.e., single metal atom doping, is carried out via anchoring to (i) metal oxide, (ii) metal surfaces, and (iii) graphene (**Fig. 3b**)[51]. Although a satisfactory progress has been made in this field, research in this area still remains elusive due to the difficulty in the control of position and valence of co-catalysts at the atomic level. In addition, understanding of atomistic mechanism of action is also elusive.

In this regard, single-atom catalyst (SAC) came forward and offered a representative platform to support and perform those activities since 1995[52-54]. SAC is unique and its enhanced performance can be obtained by properly tuning the local atom in the host configuration[50]. However, the inherent merits of SACs are that they can fill the gap between the heterogeneous and homogeneous catalytic activity. The unique properties of single atoms, such as their well-defined electronic structures, unsaturated coordination and free surface energy, make them an active center for enhancing catalytic activity in a wide range of reactions[55,56]. However, the synthesis of single metal atoms is tricky, as they can agglomerate easily.There remains a big challenge choose the right support that can promote high atomic dispersion of these single atoms[57]. Proper and stable supports are needed to stabilize them as single atoms that can always have strong interactive forces between atomic metal species and their neighbouring atoms (**Fig. 3c**). In general, through proper SAC synthetic routes, maximum utilization of the atomic efficiency can be obtained by coordination with proper supports[46,50]. The support materials should be able to reinforce the single atom and should offer high stability in a harsh environment. As a support material for SAC preparation, different inorganic compounds such as metal surface, metal nitride, metal oxides, metal chalcogenides, bi-tri-metal inorganic supports and CBMs have been studied. For example, different metal oxides such as CeO_2, Fe_2O_3, TiO_2, SiO_2, Al_2O_3, ZnO, and MgO have been employed as a ligand to anchor single atom metals (such as Cu, Pt, Au, Co, Zr, Ti, Ni, Rh and so on) to be used as an effective photocatalyst[58]. In the synthesis of single metal atom catalyst onto metal oxides support, it is necessary to create a vacancy in the molecular structure of metal oxides which can serve as an active site to bind the single atom for increasing stability. However, one of the big challenges in sintering single atoms in metal compounds is that the high loading of single atoms via a simple method at large scales is not feasible.

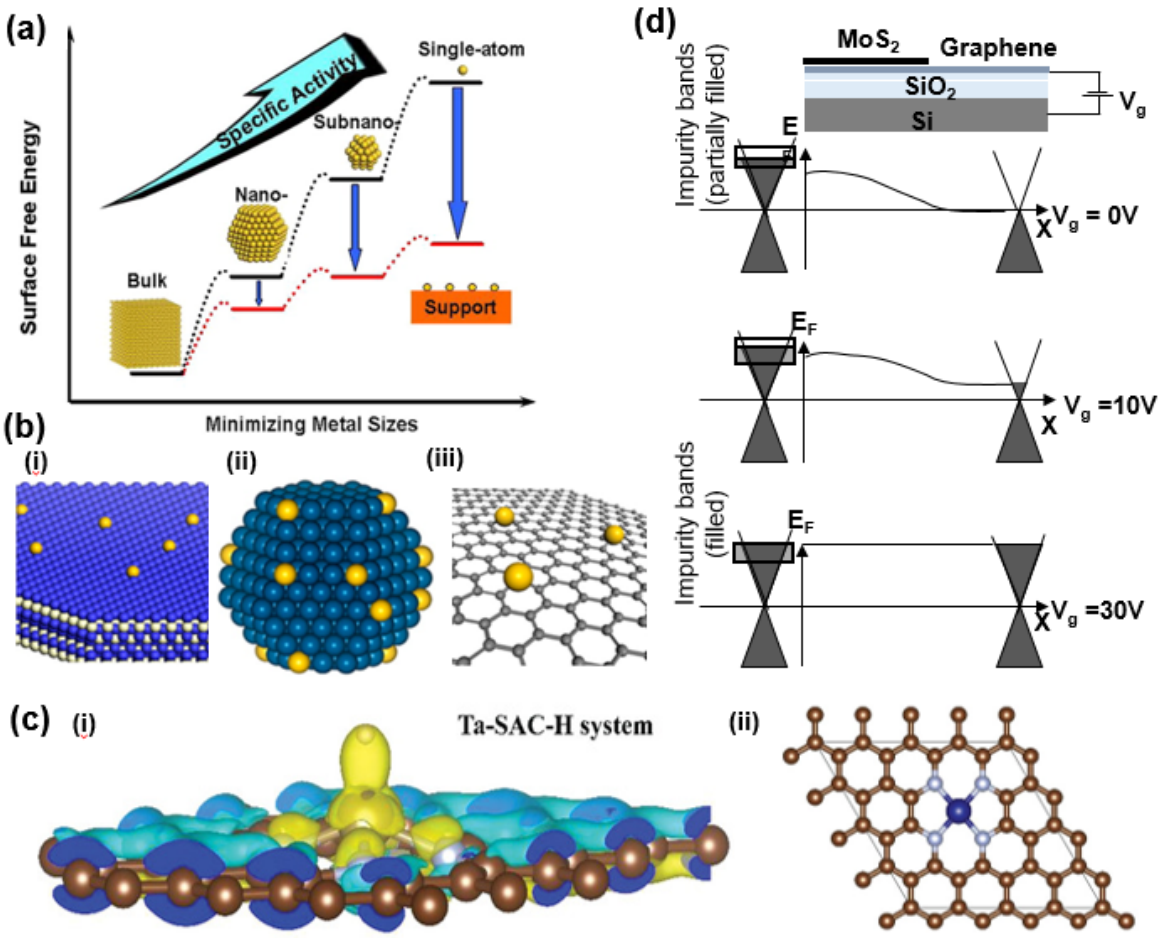

Fig. 3: (a) Schematic illustrating the changes of surface free energy and specific activity per metal atom with metal particle size and the support effects on stabilizing single atoms[51]. **(b)** Schematic of different types of SACs: metal single atoms anchored to (i) metal oxide, (ii) metal surfaces, and (iii) graphene[51]. **(c)** Charge transfer from Ta-SAC to hydrogen during the reaction (yellow color represents electron availability while blue is for electron deficiency (c-i); and metal active site coordinated with four nitrogen atoms in graphene sheet (c-ii)[56]. **(d)** Illustration of the Fermi level evolution along the MoS_2 edge for different gate voltages V_g. In the MoS_2-covered region (left), the Fermi level becomes pinned due to impurity bands while it increases in the uncovered region (right) with V_g [59].

It is worth mentioning that SAC can be well anchored if the support materials have some specific properties, including high surface free energy with a large surface area, functional groups, strong thermal stability, and high conductivity to prevent agglomeration of a single atom in the supportive media[48]. Among them, CBMs have many features such as a large surface area,

excellent electrochemical properties, low cost, high conductivity and high durability over a range of harsh environments. Therefore, CBMs are the ideal candidate to serve this purpose. CBMs, especially graphene, CNT and heteroatom doped examples, have been extensively used as supports for SACs preparation. However, fabrication of SACs on CBMs support is not an easy task, as metal atoms are very unstable and tend to aggregate during the preparatory processes due to their high surface free energy. There are many processes to produce SACs, but wetchemistry-based techniques such as defect engineering, spatial confinements strategy, and coordination design strategy are mostly used. Other processes include atomic layer deposition, high temperature vapor transport, photochemical method, pyrolysis and thermal activation, one-pot synthesis, photochemical reduction, electron/ion irradiation, and direct synthesis using different precursors such as graphene oxide (GO), molecular or polymeric precursors, covalent organic framework, metal organics framework precursors and so on[46,48,53]. Nevertheless, the main principle is that the high stability SACs with unique properties can be obtained by the strong interactions between anchored supports and single metal atoms[60]. Different computational methods are used to study the stability and interaction between the metal-carbon structures; change in Fermi level and spin density of the CBMs by doping with these metal atoms[61,62]. Especially, the first-principle methods based on different DFTs[63,64], generalized gradient approximation (GGA)[65,66], charge density difference (CDD) plotting, density of states (DOS) analysis are mostly used nowadays to investigate these features of doping. For instance, it has been found by the total density of states (DOS) and partial DOS analysis in many studies that the *d*-orbital of the TMs plays an important role in enhancing the MSIs. In a study by Tang et al.,[67] the Pt-*5d* states were found to overlap well and hybridize with the broadened TDOS states of the Pt/D-graphene systems near the Fermi level (E_F) which increases the stability of the system compared to the Pt/pure-G adsorption bonds. Furthermore, DFT-based computational methods are used to explore the active sites of the carbon-supported SACs as well as to predict the mechanism of their involving reactions such as water splitting, ORR, OER etc.[68,69]

SACs are able to provide more information on the fundamental atomic level mechanism and provide an important role in boosting the performances which can be further extended into a new angle of research in order to boost the performance as a catalyst. It can be summarized that the electronic properties, as well as the geometry of single metal atoms, mostly rely on the

properties of supports and metal atoms. In this case, CBMs can better serve to accumulate more amounts of a single atom in their core structure due to their defective structures which can easily be created.

2.4. Metal-Metal Compound/Hetero Atom Doping of CBMs

Heteroatom doping of CBMs (such as B, N) induces electron modulation of CBMs, provides necessary electronic structure, and enhances its catalytic activity and other applications. Similarly, CBMs can be an ideal support for metal or metal compounds and with further hetero atoms doping,they are promising for many applications[2]. Among CBMs, graphene is a zero band gap material, and it has a vanishing density of states (DOS) at the Fermi level. Therefore, graphene can exhibit metallic behavior as a result of its topological singularities at the K points in the Brillouin zone[70], where valence bands and conduction bands touch in conical points. Such zero band materials with metallic (or insulating) compounds or metals can alter the whole electronic properties. This happens due to the change in Fermi level to move away from the conical points. As a result, when either electron donor or acceptors (holes and electrons) induces in such kind of structure, then the doping type and concentration of doping determine the degree of shift of Fermi level with respect to the conical points[59,70]. Graphene has been doped with n-type metal atoms such as Al, Cu, and Ag, and p-type on Pt and Au to shift the Fermi level[70]. For example, the potential barrier changes when a gate voltage (V_g) is applied. Then the local Fermi level is changed accordingly as shown in **Fig. 3d**. This happens due to the MoS_2 on graphene which can partially screen the gate induced electric fields as a result of quantam capacitance related charge redistributions from graphene to MoS_2. Thus, the gate voltage-induced changes of the Fermi level are much smaller in the uncovered area than in the covered region[59]. Based on this principle, different CBMs hybrids have been synthesized, such as graphene-MoS_2[59], Ni-C-N[71], Pt-alloy supported by CNT catalyst[72], Co/CoO-graphene[73], FePt-graphene[74] and so many. It was found that transition metal and transition metal carbides, for example, NiC, have a low energy barrier and are found to be indispensable to catalyzing many reactions by forming a highly graphitized carbon hybrid. Moreover, their DOS is near the Fermi level, which is almost near to noble metals. Similarly, other transition-based metal compounds are very potent for doping with CBMs. In some studies, CBMs have been doped with different transition metal

clusters. For instance, Yan et al.[75] doped a Pt-cluster (Pt_4) into a defective graphene structure. From the PDOS analysis, they found the overlapping of the *5d* orbit of Pt with the C-*2P* orbit around the vacancy, conforming the strong interaction between anchored single vacancy graphene-Pt_4 cluster. Notably, the DOS analysis has been a popular way of analysing the states of electrons occupying the corresponding energy levels of the doping system. However, a more insight about the contribution of each energy levels to the specific atomic orbits can be obtained by the projected density of states (PDOS) analysis. Wang et al. [76] performed a theoretical study to gain insight on the change in electronic properties of MPt_{12} clusters (M = Co, Fe, Cu, Ni, Pd) when embedded in N-doped defective graphene structure. The *d*-states interaction between the Pt and N atoms for deposition of the clusters was affirmed via PDOS analysis.

Furthermore, the catalytic activity of metal-doped CBMs can be increased by doping with another hetero atom, such as nitrogen, phosphorous, sulfur etc.[71,77] Especially, the atomically dispersed transition metal SACs on these non-metallic heteroatoms doped carbon matrices have attracted considerable attention in recent years for their high catalytic performances in different reactions such as CO_2-fixation, OER, ORR, water splitting etc.[78,79] One possible source can be the facile transfer of electrons from the *d*-orbital of the TMs to its neighboring non-metallic atoms (such as N, P, S) which is easiler than the direct transfer of electrons to the pure carbon matrix. Regarding this interaction, it is possible to synthesize more carbon supported SACs in future with different structural combinations for catalytic reactions, by controlling the dopant concentration and doping processes.

3. Structure-Activity Relationship of CBM Doping

3.1. Electron Affinity

CBMs are primarily composed of mostly carbon and other elements such as hydrogen, oxygen, nitrogen, and other trace elements. The introduction of other heteroatoms such as boron, nitrogen, phosphorous, halides, oxygen-containing functional groups into CBMs could cause an electronic modulation into the overall structural conformations. Therefore, the newly orientated structure can tune its optoelectronic properties and its chemical activities, which are very useful for many applications[13,80,81]. The replacement of some carbons in the graphitic unit of CBMs

with other heteroatoms (the atoms which have higher or lower electron negativity) can show structure change induced by doping (**Fig. 3b**). A graphitic illustration based on the different parameters such as electronegativity, nuclear spins, and atomic size distribution of the commonly used dopants in CBM is shown in **Fig. 4**. According to **Fig. 4**, many elements such as N, B, P, S, O, halides and metal atoms can be enclosed in the CBMs surface through doping. Therefore, the size and electronegativity of those elements play a significant role in the electron modulation to change the overall charge distribution and electronic properties of CBMs. The larger the electronegativity difference between carbon elements increases the chance of becoming carbon more electropositive and vice versa. Similarly, larger metallic atoms in the graphitic lattice can bring more structural distortion to the CBMs surface. Hence, different defects are being created in CBMs, which could further change the chemical activity of CBMs directing too many novel applications, especially as catalysts and electrode materials.

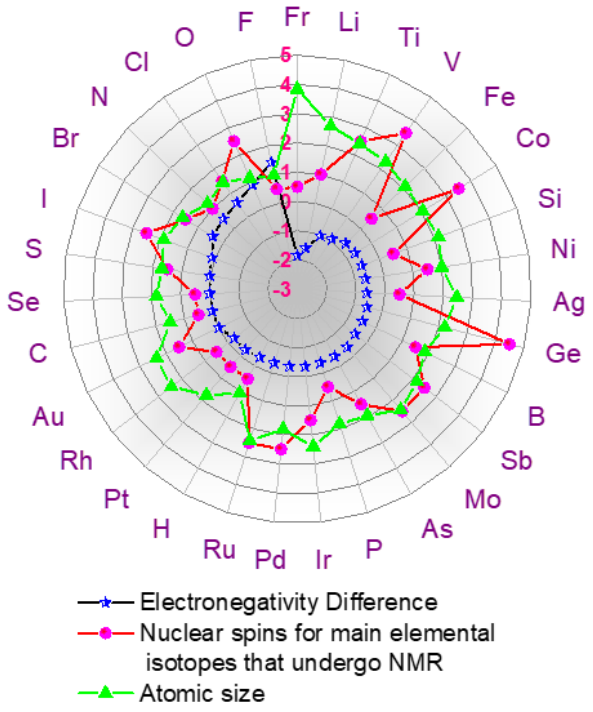

Fig. 4: Electronegativity, nuclear spins, and atomic size distribution of the commonly used dopants in CBMs.

3.2. Band Gap

The distance between the valence band, i.e., the lower energy level of electrons and the conduction band, i.e., higher energy level, is known as a band gap. The band gap is the minimal energy required to excite an electron or allow electrons to become free to a condition in the conduction band where it can conduct. Most electronic application of CBMs is hindered by their large band gap (e.g., diamond) and the absence of a semiconducting gap (e.g., pristine graphene or graphite). Therefore, reducing or opening a sizable and well-tuned band gap in CBMs is a significant challenge for carbon-based electronic devices. As a result, hetero atom doping in CBMs could be the most feasible method to control the band gap as well as its semiconducting properties. For example, CNTs usually behave like metals or semiconductors, which depend on their particular geometry or chirality[82,83]. Different electronic configurations of the doping atoms are the main cause of these various states.

Band structure changes of graphene with different heteroatoms are shown in **Fig. 5**. Substitutional doping of hetero atom, especially B and N, within graphene nano-cylinders, in particular, introduce strongly localized electronic characteristics in the valence or conduction bands and will increase the number of electronic states at the Fermi level depending on dopant position and concentration[84]. From different literatures, heteroatoms such as N, B, P, P-N etc., are among the most studied dopants used in semiconducting CNTs to tailor their physical and chemical properties by creating new states that modify their electronic structure. For instance, the introduction of the B into the surface of single-walled CNTs narrows the band gap; consequently, nanotubes possess metallic properties[32]. On the other hand, doping semiconducting CNTs with N (with excess valence electrons) atoms induces new electronic states and makes all N-doped semiconducting nanotubes to be metallic because the Fermi energy in the nanotube is shifted near to the conduction bands (**Fig. 5a (i-ii, vi-vii)**)[82]. However, pyridinic-like nitrogen doping of CNTs produces localized states in the valence bands and shifts the Fermi level to their domain **(Fig. 5a (iii, viii))**, causing them to behave like a p-type semiconductor,although, pyridine-type N may produce either a p- or n-type conductor, depending on the doping level [84]. Moreover, P similarly contains five electrons in its valence shell, but still it bonds with sp^3 hybridization, leading to trigonal pyramidal coordination, generating a localized state associated with the extra electron (compared to C) when attached to a graphitic network. As can be

observed in **Fig. 5a (iv, ix)**, this localized state appears as a practically nondispersive state, i.e. a flat band in the band structure. These P- related states do not contribute electrons to the conduction bands due to their localized nature, so they do not affect the intrinsic semiconducting or metallic properties of the nanotubes. But co-doping of P and N in CNTS affects their semiconducting properties, as two states are created near the Fermi energy, as observed in **Fig. 5a (v, x)**. The first state has a strong localization (though not as strong as the P-doped instance), but the second state mixes well with the carbon network π-electron system. These states have low dispersion and reduce the bandgap to half that of the corresponding pristine semiconducting zigzag nanotube.

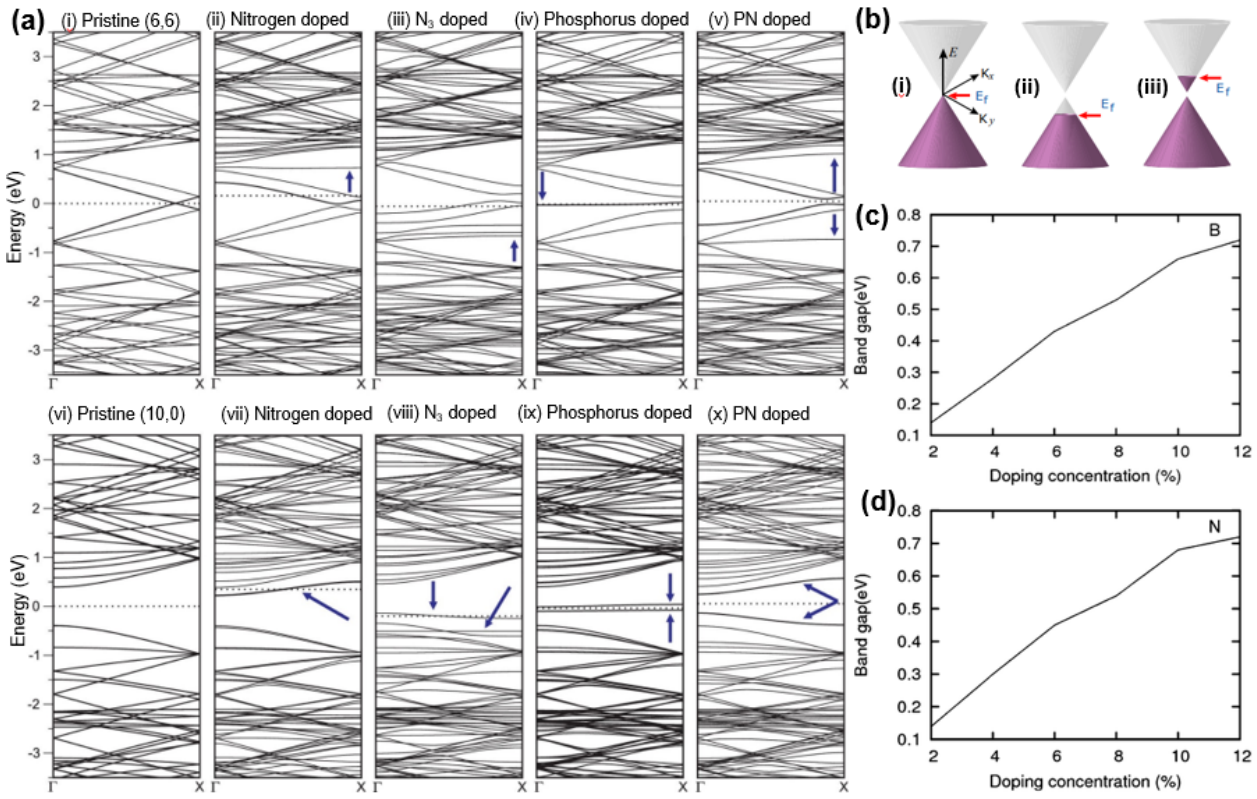

Fig. 5: a) Band structure of pristine and doped (6,6) armchair metallic nanotubes (top) and (10,0) zigzag semiconducting nanotubes (bottom): (a,f) pristine, (b,g) nitrogen doped, (c,h) N3 doped, (d,i) phosphorus doped, and (e,j) phosphorus nitrogen doped. The presence of localized states around the defects is reflected as the low dispersion bands indicated by arrows. Notice that the bands are dispersion less in the phosphorus-doped cases,indicating strong localization [82]. **b)** Schematic band structures of graphene. **(i)** Band structure of pristine graphene with zero

bandgap. E_f is at the cross-over point. Band structures of **(ii)** *p*-type and **(iii)** *n*-type graphene with the bandgap. E_f lies in valence and conduction band, respectively [85]. (E_F=Fermi Level) **c)** Band gap in increasing order of doping concentrations for a boron doped graphene sheet[86]. **d)** Band gap in increasing order of doping concentrations (for the configuration having a maximum band gap) for N[86].

Graphene-based electron devices face a tremendous barrier in opening a sizable and well-tuned bandgap as it has zero-bandgap. **Fig. 5b(i)** shows the schematic band structures of pure graphene around the Dirac point with a linear energy-momentum dispersion relation ($E = \pm h\nu|\mathbf{K}|$, where ν is the Fermi velocity) [87]. It has cone-shaped valence and conduction bands that meet at the Brillouin zone's K point. **Fig.s 5b(ii)** and **5c(iii)** show the schematic band structures of p- and n-type graphene, respectively, with the bandgap and Fermi levels (E_f) in the valence and conduction bands. The influence of substitutional doping on the structure and electrical characteristics of graphene was investigated using first-principles density functional theory (DFT) and ab initio calculations[88]. The results have shown that with B- and N-doping, the linearity in the dispersion of electronic bands within 1 eV of the Fermi energy is nearly unchanged, implying that doped graphene has a band structure with a linear dispersion relation comparable to pure graphene. Nonetheless, after substitutional doping with B and N atoms, the bandgap in graphene is opened, and the Fermi level lies in the valence and conduction bands, respectively, exhibiting ideal p- and n-type semiconducting electronic properties as shown in **Fig. 5b (ii-iii)** for potential applications of graphene in electronic devices. Another theoretical study[86] has found that the electrical properties of a graphene lattice are symmetrical and that the placement of dopant atoms (B & N) influences the band gap. It was also observed a proportional relation between band gap and doping concentration, as shown in **Fig.s 5c-d**. Moreover, the S and Si (least effective) doping open or tune the band gap of graphene and graphene nanoribbons, respectively[89,90]. Because silicon has a higher atomic radius than carbon, the intensity of the interaction increases, resulting in a repulsive force that causes the band-gap to open. They also observed hybridization between the p orbital for both Si and C; thus, the σ band remained unaltered, in contrast to the π band. The electronic structure wass unchanged with lower Si concentrations. Due to the similarity of Si and C atoms, silicon doping in graphene structure is projected to have a less detrimental effect on graphene mobility. When the concentration was

increased (8.3%, 12.5%, 25% and 50%), the semiconductor behavior took precedence over the gapless, and the gap widened. On the other hand, other researchers observed that co-doped CBMs were usually more electrocatalytically active by reducing the band gap[91,92]. They investigated that additional doping of boron or phosphorus in nitrogen-doped graphene could lower the energy gap of N-doped graphene materials.

So, it can be concluded that doping of heteroatom within CBMs will introduce strongly localized electronic features in the valence or conduction bands and will enhance the number of electronic states at the Fermi level depending on the location and concentration of dopants. As a result, the band gap of CBMs is reduced or expanded (**Table-1**) which enhances the electronic properties as well as the catalytic activity.

Table 1:

Fermi Energy (E_f) and Band Energy (E_g) of pure carbon materials and doped carbon materials.

Carbon Materials			E_f (eV)	E_g(eV)	Ref
(8.0) Nanotubes	Pristine CNTs		0.16	0.61	[32]
	B-doped CNT (7.8 at%)		0.64	0.35	
(10.0) Nanotubes	Pristine CNTs		0.15	1.03	[32]
	B-doped CNT (6.25 at%)		0.61	0.30	
(10.0) Nanotubes	Pristine CNTs (C_{40})		0	0.75	[93]
	BC_{39}		0.020	0.44	
	BC_{79}		0.021	0.57	
	BC_{119}		0.022	0.62	
	B_2C_{78}		0.057	0.49	
(10.0) Nanotubes	Pristine CNTs		-	0.8	
	PN-doped nanotubes		-	0.38	
Carbon Nanotube	Pristine CNTs	Metallic CNTs	-	0	[94]
		Semiconducting SWNTs	-	0.767	
	N-doped CNTs	N_Q (Quaternary) CNTs	-	0	
		N_P (Pyridinic) CNTs	-	Open	
Graphene	Pristine graphene			0	[95,96]
	N-doped graphene			0-0.2	
	Monolayer			0.42-2.43	[97]

BN co-doped Graphene	Bilayer	0.11-2.20	
	Trilayer	0.04-2.08	
	Multilayer	0.02-1.90	
	Superlattice	0.08-0.20	
Graphene	Pristine Graphene	0	[90]
	Si-doped Graphene	1.022-3.43	

3.3. Spin redistribution

Insertion of heteroatoms (e.g., N, B, P, S, X etc.) in CBMs with different sizes and electronegativity could further cause electron modulation to provide desirable electronic structures for many catalytic processes of practical significance[98]. Doping can cause structural changes by replacing certain carbons in the graphitic unit of CBMs with different heteroatoms, which are higher or lower electron negativity. As discussed earlier, the size and electronegativity of dopant elements play an important role in the electron modulation to change the overall charge distribution and electronic properties of CBMs, which could further change the chemical activity of CBMs, resulting in many novel applications, particularly as catalysts and electrode materials. Heteroatom doping of carbon nanomaterials has been proven to generate charge and/or spin redistributions, which could be a potential strategy for developing metal-free, carbon-based catalysts with greater electrocatalytic activity and better long-term operating stability. Yang et al.,[99] revealed based on DFT calculation that the intrinsic catalytic activity of hetero atom doped graphene on the ORR mechanism. They stated that the charge, the spin density, and the coordinate state (ligand effect) of the carbon sites greatly affect the catalytic activity.

The doping-induced charge polarization or redistribution due to the difference in electronegativity between carbon and heteroatom dopants, which have higher (as N) or lower (as B) electronegativity than carbon (**Fig. 4**), could create charged sites (C+ or B+) which are favorable for O_2 adsorption to facilitate the catalytic process. But when the difference in electronegativity between carbon and doped heteroatom is very low or negligible (as Se, S), the change of atomic charge polarization or redistribution is relatively much smaller[100]. Therefore, doping-driven spin redistribution must have contributed to the improved catalytic activity of S or Se-doped CBMs because of the difference in electronegativity between carbon (χ= 2.55) and sulfur (χ=2.58) or selenium (χ=2.55) is almost negligible[92]. In contrast to F and N, the impact of S in increasing catalytic activity was linked to the high spin density on neighbouring carbon

atoms (**Fig. 6a**)[101]. Zhang et al.,[102] identified the catalytic active sites on single N-doped graphene, which have either high positive spin density or high positive atomic charge density (**Fig. 6b**). They indicate that the doping-induced charge and spin redistributions are crucial in improving the ORR electrocatalytic activity of N-doped graphene. This group have concluded that spin density plays a significantly larger role in identifying the catalytic active regions in doped CBMs than atomic charge density.

On the other hand, Qiao and co-workers observed the combined effect of doping-induced charge transfer and spin redistribution in N and S co-doped CNTs[103]. The resulting N, S co-doped CNTs exceeded most previously reported carbon nanomaterials in terms of catalytic activity as bifunctional catalysts for both HER and OER. According to theoretical estimates, secondary S element doping resulted in a large spin density redistribution in the co-doped model structures, leading to a considerable increase in the number of carbon atoms to be used as active sites to adsorb H* and OOH* electrocatalytic intermediates, and therefore increased the HER and OER activity. Therefore, carbon atoms with either high spin densities and/or positive charge could serve as the active sites, which promoted the chemical activity of heteroatom doped-CBMs. If the negative spin density is low, carbon atoms with a high positive atomic charge density may serve as active sites.

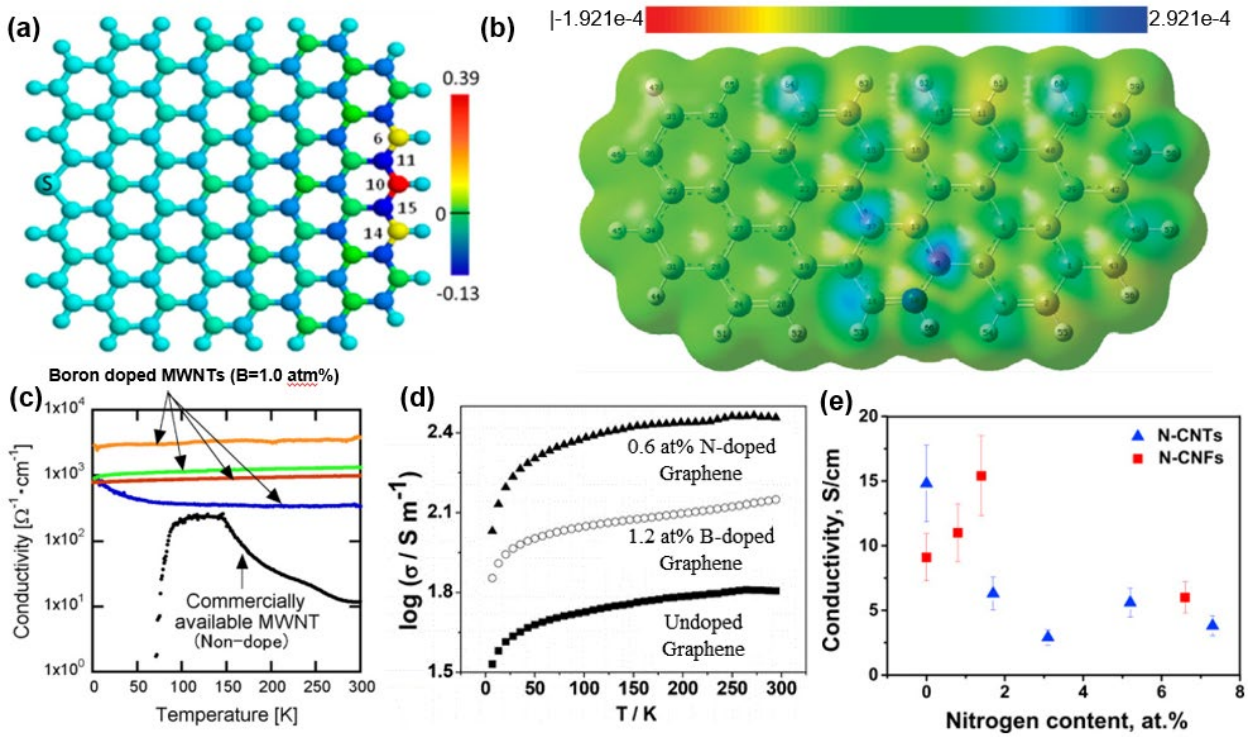

Fig. 6. (a) Spin density distributions on S-doped graphene at the zigzag edge[101]. b) spin density distribution on the N-graphene with pyridine structure ($C_{45}NH_{20}$)[102], The electron density isovalue plane displays the distribution of spin density; the most negative value is represented by red, and the most positive by blue. (c) Boron-doped MWNTs show higher conductivity than commercially available MWNTs, even at very low temperatures[104]. (d) Temperature dependences of electrical conductivity of N- and B-doped graphene[10]. (e) Dependence of electrical conductivity on the nitrogen content in N-CNTs and N-CNFs[105].

3.4. Conductivity of Doped Carbon Materials

The ability of an electric charge or heat to move through a material is measured by conductivity. A conductor is a material that allows an electric current or heat energy to flow with extremely minimal resistance. The electrical and thermal conductivity are inextricably linked. Strong electrical conductors are typically also good thermal conductors. CBMs have relatively good thermal, electrical, and ionic conductivity characteristics[106]. The conducting capabilities of CBMs such as CNTs, graphene and others, can range from metal to semiconductor depending on

structural features and heteroatoms such as N, P, S, B, and etc., doping[107]. The dopants whose electron affinity and electronegativity are different from those of the carbon atoms are introduced in any CBMs, resulting in the perturbation of the electron distribution, leading to higher charge delocalization, change of hybridization, and change of conjugate structures in the materials. Various precursors and synthetic methods have been worked to make heteroatom-doped carbon materials with different structures such as graphene, graphite, CNTs, mesoporous carbon etc., the different densities of dopants and different types of dopants and dopant species[108,109]. These structural features of the materials affect the electrocatalytic properties, such as the electrocatalytic activity and electrical conductivity[110]. For instance, doping with alkali metals enhances the conductivity, e.g., producing superconductivity of fullerenes, diamond and graphite. Undoped diamond is an insulator, but the diamond has been turned up to become a superconductor after it undergoes a metal-insulator transition by B-doping [111]. For example, Ishii et al. [104] doped B in CNTs to enhance their conductivity. It was found that the conductivity of B-doped multi-walled CNTs (MWNTs) maintained high conductivities of 10^2-10^3 $\Omega^{-1}cm^{-1}$ **(Fig-6c)**. Inagaki et al.,[10] observed that B-doping, e.g., hole-doping was much less effective than N-doping, e.g., electron doping in graphene to improve electrical conductivity (**Fig. 6d)**. Among other heteroatoms, N can occupy different sites during its incorporation into the carbon structure. Three categories of nitrogen dopants exist in nitrogen-carbon materials including graphitic (quaternary) N, pyridinic N, and pyrrolic N, among the graphitic N species, which could effectively improve the electrical conductivity of the carbon matrix[112]. Based on the theoretical aspect, incorporating more electron-rich N into the sp^2 carbon matrix could donate electrons to the delocalized π-system, increasing the localized density of states at the Fermi level and leading to enhanced n-type conductivity[113]. N-doping within a certain range can increase the electrical conductivity of carbon nanomaterials, i.e., the conductivity of NC materials changes nonlinearly with the nitrogen concentration (**Table 2**). As seen in **Fig. 6e**, doping has both positive and negative impacts on the electrical conductivity of N-CNTs. For example, Ismagilov et al.,[114] observed that the maximum electrical conductivity at an intermediate nitrogen concentration equaled to 3.1 wt.% and the lower conductivity nitrogen concentration in N-CNFs equaled to 8.2 wt.% at ambient temperature. So, it has been concluded that quaternary nitrogen is responsible for the increase in conductivity for most of CBMs.

Moreover, CBMs co-doped with multiple different hetero atoms is currently of great interest due to their higher boosting ability of conductivity than mono hetero atom doped carbon materials. For instance, N-doped activated carbon showed lower electrical conductivity than N/P co-doped activated carbon[115]. P is more capable than N of influencing the electronic structure of carbon materials (act as electron donor) due to their large radii than a carbon atom. Also, adding more electron-rich N to the C network could bring more electrons to the delocalized π-system of carbon materials, resulting in increased electrical conductivity; substitutional P and P/N doping creates localized electronic states that modify electron transport properties by acting as scattering centers. So, it can be concluded that doping of heteroatom in CBMs affects the electronic structure of carbon materials by bringing more electrons to the delocalized π-system of carbon materials, resulting in increased electrical conductivity. It can be also summarized that hetero atom co-doped CBMs showed high electrical conductivity than mono-hetero atom doped CBMs.

Table 2:

Conductivity of some doped carbon based materials.

Doped CBMs			Concentration of doped element (%)	Conductivity [$\Omega^{-1}cm^{-1}$]	Ref
CNMs	N-CNTs		2.7	12.5	[116]
	CNT	Pristine		$0.17\text{-}2\times10^{5}$	[94]
		N doped-CNT mat		219	
	N-SWCNTs		0.4	1800	[117]
			1.6	1000	
	N-CNFs		0	9.1	[114]
			1.7	11.0	
			3.1	15.4	
			8.2	6.1	
	N-mesoporous carbons		0	0.08	[118]
			4.3	0.43	
			8.1	0.26	
			11.9	0.04	
	N-CNTs mats		0	258	[119]
			4	325	
			5	123	

		6.3	53	
		7.4	60	
B-CMs	B-MWCNTs	1.0	10^2-10^3	[120]
Graphene	Pristine graphene		10^6	[94]
	N-doped graphene		8333	
Activated	Pristine C-Blank		0.01276	[115]
Carbon	C-N		0.01706	
	C-N/P		0.02551	

4. Role of Orbital Chemistry in Doping

4.1. Role of Orbital in Doping

The catalytic function of doped carbon materials is highly dependent on the electronic structure of that materials. Depending on various quantum chemical characteristics like electron density, band gap, density of states (DOS), and partial density of states, the fate of one material could be determined as a good material or not. Among them, the re-arrangement of electron charge density due to the addition of doping materials strongly influences the catalytic ability of a material. The dopant stimulates a local change in electron charge that plays the most influential role in reactivity[121]. This significant variation of local charge of the molecule would eventually induce an orbital hybridization of highest occupied molecular orbital (HOMO) of the pristine molecule and lowest unoccupied molecular orbital (LUMO) dopant atom that consequently reduces the energy gap between the ground state and excited state of the doped molecule[122]. It's worth mentioning here that the difference between HOMO and LUMO is expected to be small for for a molecule to be reactive as this energy is needed to overcome for electron excitation[123]. The HOMO–LUMO energy difference calculated using DFT for various doped carbon-based molecules that exhibits the lower energy gap to be supportive for catalytic actions that are illustrated in **Fig. 7**. The HOMO–LUMO energy gap is displayed in **Fig. 7(a)**, and the the absolute hardness η can be gaussed from the energy gap, as $\eta = (\varepsilon_{LUMO} - \varepsilon_{HOMO})/2$, where ε_{HOMO} and ε_{LUMO} are the energies of the frontier orbitals as higher energy gap implies higher hardness, i.e. the inertness. Lowered hardenss helps the doped molecules to show higher catalytic activity than the pristine one. On the other hand, **Fig.s 7(b-f)** exhibits the contribution of hetero atoms in molecular orbital rearrangement. N and Cl atoms having higher electronegativity than carbon

atom attact electron toward them upon mono hetero atom doping, whilst S, B and Si have similar or less electronegativity, and exhibit orbital hybridization upon di-hetero atom doping.

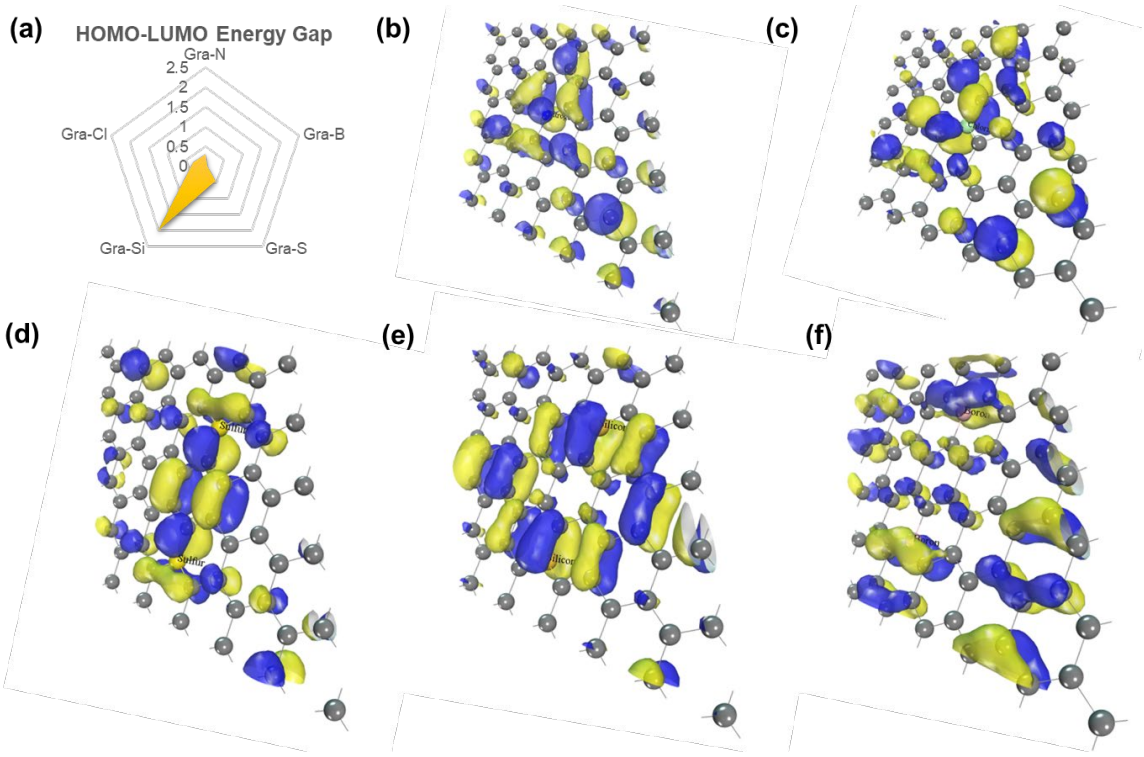

Fig. 7: (a) HOMO-LUMO energy gap, HOMO of (b) N doped graphene, (c) Cl doped graphene, (d) S doped graphene, (e) Si-doped graphene, and (f) HOMO of B doped graphene; respectively.

For the purpose of describing the electrical characteristics of solids and for qualitatively assessing optical, photoelectron, transport, and other types of experimental data, the partial density of states (PDOS) functions are another computational approach of vital significance. PDOS postulates the orbital interactions and qualitative charge transfer behaviors. So, PDOS is extensively used by researchers to postulate the interactions of CBMs and dopants. For example, Kim et al.,[124] showed PDOS along with electron density of 2p orbital of N-doped graphene. They found electron accumulation near that orbital from the electron density plot and PDOS graph simultaneously. Yadav et al.,[125] also reported similar results of PDOS for Zr-doped graphene that

there is a dislocation and redistribution of electrons by the introduction of Zr atom in graphene. The PDOS plots of the density of states of C-2p orbital for graphene and the N-doped graphene is illustrated in **Fig. 8a**. The augmentation of partial density of states of C-2p orbital of N-doped graphene is seen in the PDOS graph in comparison with pristine graphene. A certain diminution of charge near the fermi level of clearly visible than pristine graphene and N–deopd graphene which suggests a certain amount of charge has been shifted from C atom to N atom[126]. This indicates the stimulation of graphene via dopant atom could help to achieve better chemical reactivity. In conclusion, DFT studies on several hetero atoms doped CBMs have confirmed that there is a change in charge among orbitals while a CBM is doped, which enhances the catalytic capabilities of the material.

4.2. Role of Sub-Orbitals in Doping

As was already established, a doped molecule's electronic structure significantly affects both its physical and chemical properties. In this sense, researchers are particularly interested in defining the contribution of sub-orbitals in this area in order to determine their precise properties. The partial density of states of sub-orbitals is a widely used indicator to comprehend the subsidy of sub-orbitals for CBMs and doped CBMs. For example, Gangan et al.,[127] discussed the suborbital contribution of Y-doped Graphene (acetylene linkage). The isolated Y atom is magnetic in nature and only d_{z2} was seen to be occupied while Y got absorbed by graphyne, charge is redistributed across different sub-orbitals as a result of a charge transfer from Y to graphyne. The 5s and 4d states of the Y atom have both been pushed above the Fermi level (i.e., become unoccupied) when comparing the PDOS of Y-doped graphyne with that of the isolated Y atom. This shows that there has been a charge transfer from both of these states to graphyne. Now, d_z^2 and d_x^2-$_y^2$ are less occupied and empty d_{xy},d_{yz} and d_{xz} in isolated Y have now become partially occupied that suggest that upon absorption, d_z^2 and d_x^2-$_y^2$ suborbitals of Y atom transferred certain charge to carbon and rest of the suborbitals got occupied indicating the involvement of all suborbitals on binding. **Fig. 8c** illustrates the PDOS of d orbital for the isolated Y and graphene-Y system[127].

On the other hand, Chakraborty et al.,[128] also postulated a similar scenario for 3d sub-orbitals of Ti-doped Ψ graphene. The phenomenon of charge re-distribution is also experienced

in this case. The d_{xy}, d_{yz} and d_{xz} sub-orbitals are occupied when Ti is isolated where there is no state of the valence band in $d_{x^2-y^2}$, d_{z^2} is observed. But upon doping, $d_{x^2-y^2}$, d_{z^2} sub-orbitals become partially occupied by the valence band while d_{yz} got unoccupied. This redistribution of charge in Sub-orbitals also role significantly in catalytic activity. **Fig. 8b** shows the PDOS of d-orbitals of isolated Ti, and Ti in a graphene system.

The above discussion shows a brief picture of the contribution and involvement of suborbital in determining the characteristics of of doped CBMs that how the redistribution of charge among suborbitals creates the foundation of improved properties in the doped materials. Improvement of compuatational approaches and quantum chemical functional would certainly discovers more in-depth knowledges about their benefaction in this sector

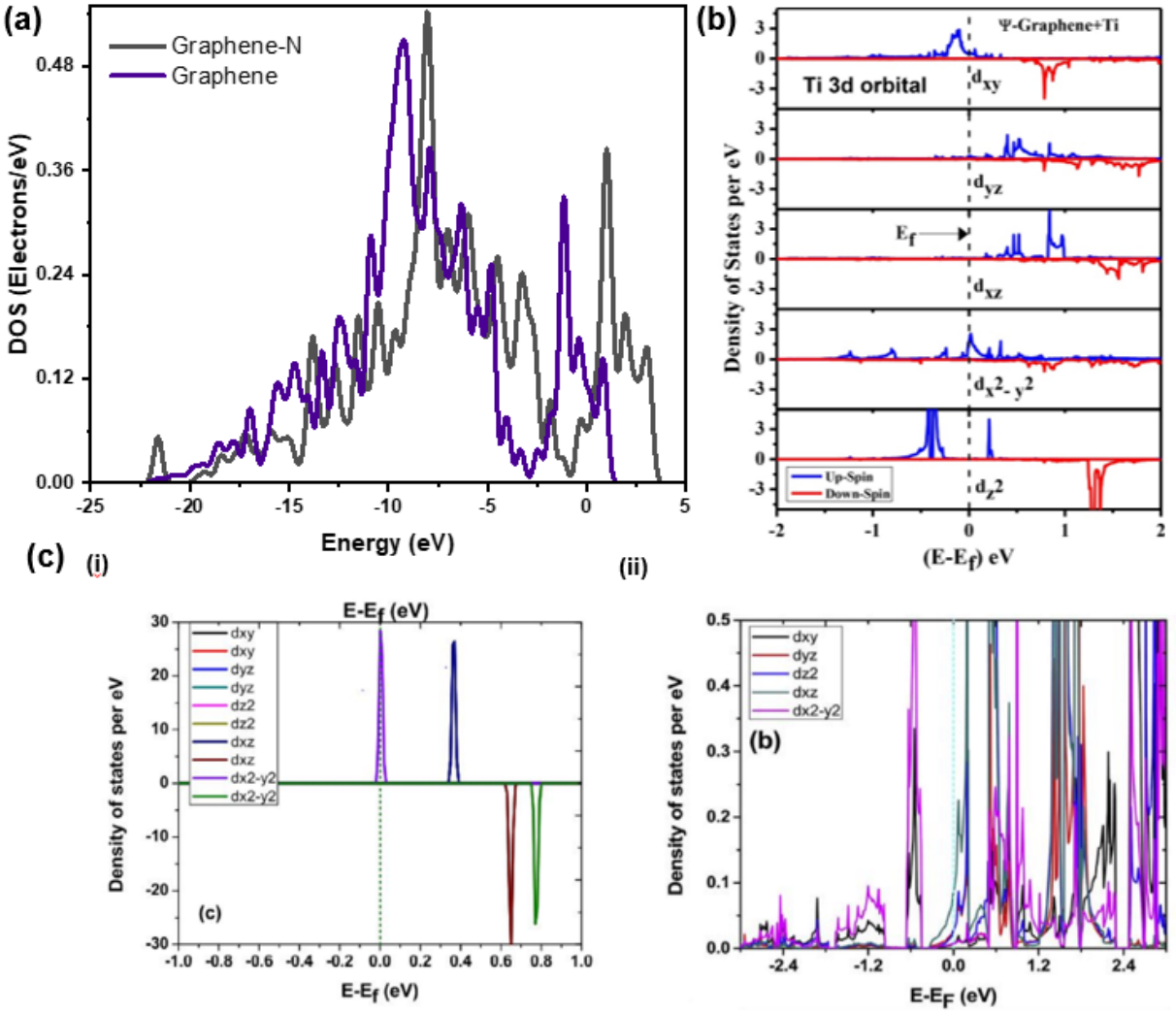

Fig. 8: (a) The PDOS plots of density of states of C-2p orbital for Graphene and N-doped Graphene. (b) Partial Density of States of sub-orbitals *dxy, dyz, dz^2, dxz*, and dx^2- y^2 of the 3d atomic orbital of Ti in Ψ-graphene +Ti[128]. (c) PDOS of (i)d orbitals of isolated Y atom; and (ii) Y d orbitals for graphyne-Y system[127].

5. Nature of Bond Formation Through Doping

5.1. Covalent Bond

Carbon is an element of group-IVA with four electrons in its outermost shell. Hence, it is more likely to form covalent bonds with other carbon atoms or heteroatoms such as N, B, O, S, P, etc., by sharing its valence electrons. The importance of such covalent doping of CBMs with various heteroatoms has been widely studied. For instance, the doping of CBMs with various foreign atoms has been practiced as an effective way of anchoring various metal atoms to boost the catalysis of different chemical processes like ORR, OER, HER, CO_2-reduction reaction etc. For example, Bulushev et al.,[129] prepared N-doped carbon nanofibers (CNFs) to anchor Pt-group metals that showed promising catalytic activity for producing H_2 from formic acid. The DFT calculations revealed that the covalently bonded N-dopants in CNFs were the major active anchoring sites for the metals. On the other hand, Zhang et al.,[130] embedded Fe metals into N-doped carbons to test their ORR activity as an electrocatalyst. Two different types of covalent bonds were detected between the C and N atoms (i.e., the pyrrolic-N and pyridinic-N) via soft X-ray absorption spectroscopy (XAS) measurement. XPS is an effective tool for studying the surface electronic states, valance structure and the overall chemical state of a material[131]. Paraknowitsch et al.,[132] reported N-doped macro- and mesoporous carbon monoliths as a suitable electrode for supercapacitors and a promising electrocatalyst. Two different types of C-N covalent bonds were distinguished in the XPS profiles, i.e., quarternary-graphitic-N (401 eV)[133] and pyridinic-N (398.8 eV)[134]. The amount of an existing bond type can also be conveniently determined from the intensity of the deconvoluted curves[132]. **Table 3** represents some examples of doped CBMs for various applications.

In recent years, heteroatom-doped carbon quantum dots (CQDs) are quasi-spherical zero-dimensional (0D) nanomaterials having a diameter of less than 10 nm[135]. Especially, S and N

atoms possess almost similar electronegativity (e.g., the electronegativity of S=2.58, C=2.55) and atomic radius (e.g., the covalent radius of N=0.75 Å, C=0.77 Å), thus forming strong valence bonds[136]. Hu et al.,[137] prepared N-doped CQDs to photochemically catalyze various organic dyes such as Congo red, Ethyl violet, Bordeaux and Indigo carmine. The covalent doping between the N atoms and CQDs, which was confirmed by XPS and FT-IR spectra analysis, enhanced the quantum yield of the CQDs significantly. Pang et al.,[136] synthesized an N, S co-doped carbon dots by hydrothermal process. The presence of C–S–C, C–S and C=N covalent bonds in the doped carbon dots were detected by the XPS method in that work. The S-doped CQDs were also reported as selective and highly sensitive detectors for different heavy metals.

In conclusion, the past five decades have seen the use of covalently bonded carbon-based frameworks doped with heteroatoms for a variety of purposes. Among these works, doping of graphene, graphene oxides, CNFs, CNTs, and different carbon monoliths with N, P, S, B, and O-atoms has been mostly reported.

5.2 Non-covalent Bonds

Besides the typical covalent bonds, some non-covalent bonds in CBMs have also been reported in several research works. Among them, the coordination, semi-ionic and ionic bonds are salient. A coordination bond, also known as dipolar or dative bond, is a type of two-electron, two-center bond in which both the electrons come from the same atom and the other atom act as an electron pair acceptor[138,139]. The presence of coordination bonds in the doped-CBMs has been found in most of the metal-nonmetal co-doping systems. In recent years, atomically dispersed SACs in carbon matrices and metallic SA-doped CBMs have attracted considerable attentions as electrocatalysts for different applications such as CO_2-fixation, water splitting, fuel cells, etc. In most cases, it has been found by different analytical methods like XPS data, FT-IR spectra, energy dispersive spectrometric (EDS) mapping, as well as computational methods such as DFT calculations that the SACs are doped into the CBMs more effectively by forming coordination bonds with another heteroatom dopant of CBMs such as S, N, O, etc. For instance, Li et al.,[78] loaded Pt SACs on N-doped carbons (Pt_1/NPC) via direct UV-irradiation to boost their HER activity. A square planar-type Pt-N_4 coordination bond was detected in the XAS and XPS

measurements. Kown et al.,[79] introduced Pt SAs in S-doped carbons and demonstrated the existence of embedded Pt^{2+} centers in the CBMs that formed a coordinated Pt-S_4 configuration with two strong and two liable Pt-S bonds. The enhanced HER activity of the Pt/S-doped carbons was attributed to the transfer of charges from Pt and S to the anchoring carbon atoms and the obtained higher valance state of Pt atoms[140]. Cao et al.,[141] prepared Co-loaded P-doped g-C_3N_4, where the initial Co-N_4 coordination sites were detected via operando XAS studies. Similar moieties were also detected in another work by Fei et al.,[142]. The DFT calculations from Cao et al.,[141] unveiled that the HO-Co-N_2 moieties were the actual active sites that facilitated the water-splitting process via charge transfer from the loaded Co SACs to the coordinated OH^- and N sites. Sa et al.,[143] calculated many possible C-N_x configurations (such as Co-N_{2+2}, pyrrolic and pyridinic Co-N_4, CoPc and different Co-N_5 coordination moieties) in their prepared Co SAC-loaded CNTs. Lu et al.,[144] embedded Ru SACs and Ru nanoparticles in N-doped carbon nanowires that demonstrated a record high HER activity with a low $\eta_{10,HER}$ (-12 mV). According to the DFT calculations, most of the Ru SACs were found to be part of Ru-C_xN_y coordination sites. In another research work, Liu et al.,[145] loaded Pt SAs onto an onion-like pyrolyzed carbon support (Pt_1/OLC) via ALD method. A highly stable tetrahedral coordination structure of Pt-O_2C_1 was found on the pristine C_{295} (fullerene-like) cage surface in the EXAFS analysis and DFT calculations. A more detailed overview of such salient research works describing the presence and effects of coordination bonds between various carbon matrices and heteroatom dopants is provided in **Table 3**.

Other than the coordination bonds, there is also some evidence of heteroatom doping of carbon materials by semi-ionic bonding. The semi-ionic bonds can be considered as an intermediate state between the ionic and covalent bonding where the high polarities between the participant atoms (due to their large difference in electronegativity) result in a comparably higher negative charge on the dopant atoms[146]. For instance, Kim et al.,[147] prepared an F-doped carbon catalyst for OER. The presence of semi-ionic C-F bonds was detected in the catalysts by XPS analysis. In some previous work, the C-F covalent bonds were presented by DFT calculations which showed the sp^3-hybridization in the corresponding carbon atoms[98,148]. However, the ionic C-F bonds are observed for the sp^2-hybridized carbon atoms from graphitic structures[149,150]. In the work of Kim et al.,[147], they synthesized the F-doped carbon catalysts by using simple

pyrolysis method. The results showed that the amount of C-F semi-ionic and covalent bonds could be controlled by changing the pyrolysis temperature. The existence of some ionic bonding in heteroatom-doped (especially metal-doped) CBMs has also been reported. For instance, hydrogen is considered a significant energy carrier, although its production and storage limit its applicability for mobile applications[151-153]. The unsatisfactory H-storage capacity of undoped pure CBMs has been reported in many studies[154,155]. For this reason, researchers focused on doping of CBMs with various light-weight metals and transition metals such as Li, K, Ca, Be, Mg, Al, Ti, Sc etc.,[156,157]. Sun et al.,[158] doped Li atoms in pure fullerene ($Li_{12}C_{60}$) and demonstrated an improved H-adsorption performance of the CBMs. The charge transfers to the C_{60}-cage from the Li 2s orbital made the Li atoms positively charged, which resulted in partial ionicity.

According to the Mulliken charge analysis, it has been found that the Li atoms carry the charge of +0.5, which is almost equal to the Mulliken charge of Ni found in Ni-C_{60} cluster systems[159]. This result affirmed the presence of partly ionic bonding between the Li atoms and fullerene structure besides the conventional covalent bonds. Similar properties were also reported by Chandrakumar and Ghosh[160]. The conserved domains database (CDD) analysis is another convenient computational method to gain a more insight on the metal/heteroatom dopant complex interactions with CBMs. For instance, A theoretical study by Wang et al.,[76] showed the interaction between $FePt_{12}$ NPs and N-doped defective graphene by CDD plots. The strong interaction between the Pt atoms and anchoring N-atoms were characterized by the strong charge accumulation of the sp^2 dangling bonds of the N atoms and depletion of charges from the Pt-*d* states of the NPs. This resulted in a partial ionization of the transition metal dopants that helped to make a strong interaction between the TMs and the supporting CBMs.

Table 3:
Examples of some doped CBMs for various applications.

Heteroatom doped CBMs	Doping elements	Synthesis method	Bond formed in the doped materials	Analytical methods used to confirm the bonds	Application	Ref.
N, S co-doped carbon dots	N, S	One-pot hydrothermal method	C=O, C–S–C, C–S, C=N, pyrrolic-N, lactam-N, imide-N bonds	XPS FT-IR spectra	Fluorescence detection of metals (e.g., detection of Fe^{3+} from other ions)	[136]
Pd/N-CNFs	N	Incipient wetness impregnation process	Pyridinic-N, pyrrolic-N, graphitic-N bonds	XPS	Catalysis of H_2 production reaction from formic acid	[129]
Fe-doped hierarchical porous carbon	Fe, N, O	Template-free pyrolysis process	Fe-N-C coordination-covalent bonds	XPS EDS mapping	Enhanced electrocatalytic performance for ORR (producing peroxides as byproduct)	[161]
Fluorine doped carbon	F	Pyrolysis of precursors (i.e., nafion and EC-600JD)	C-F covalent, ionic and semi-ionic bonds	XPS	Enhanced OER activity due to the semi-ionic C-F bonds	[147]
N-doped graphene oxide	N	Ultra-sonicating mixing followed by hydrothermal treatment (in autoclave)	Pyridinic-N, pyrrolic-N, graphitic-N bonds	XPS Raman spectra XRD analysis	Selective capture of different metal ions from aqueous solutions or water	[162]
N-doped carbon	N	Thermolysis of ionic liquids	Pyridinic-N and quarternary graphitic-N bonds	XPS	Electrodes in super-capacitors and electrocatalysts for ORR	[132]
Alkaline earth metals (i.e., Mg, Ca, Sr, Ba)-doped g-C_3N_4	N, alkaline earth metals	Solubilization of precursors (thiourea and salts of AEMs) followed by furnace heating (i.e., calcination)	M-C-N_x bonds	XPS DFT calculations	Enhanced photocatalytic activity for NO removal	[163]
N-doped amorphous carbon	N	Vacuum deposition method	Pyrrole-N, graphitic-N bonds	EELS analysis	N/A	[164]

Gold and copper carbide clusters	Au, Cu	Laser vaporization	M^{n+}-C_m coordination bonds	Photodissociation mass spectra	N/A	[165]
Heteroatom doped graphene nanoribbons	N, O, F	Pyrolysis process	N-C, C=O, C-F covalent bonds	DFT calculations	Preparation of dendrite free Li-anodes that possess low Li nucleation overpotential	[166]
Sulphur doped carbon quantum dots	S, O	Hydrothermal method	C-O, C=O, -C-S-C- covalent bonds	XPS UV-vis spectra	Quantitative detection of Hg^{2+} in water	[167]
P-, N- co-doped NPMCs	N, O, P	Pyrolysis of polymerizable ionic liquid ([Hvim]H_2PO_4)	N-C=N, N-O-P, pyridinic-N, pyrrole-N covalent bonds	XPS XRD Raman spectra	Catalysts for ORR (acquired onset potential 0.92V)	[168]
Co_3O_4/CN HNPs	Co, N, O	Wetness-impregnation process and subsequent thermal annealing	Co-N coordination bond, pyrrole C-N, pyridinic C-N, C-O, O-C=O covalent bonds	XPS ICP-AES	Improved catalytic performance for OER	[130]
Pd-N_x-C nanocomposites	Pd, N	Wetness-impregnation process	C-N covalent bonds (Pyridinic-N and pyrrolic-N), Pd-N_x coordination bonds	XPS EXAFS spectra	Enhanced electrocatalytic activity for ORRs	[169]
Fe-doped g-C_3N_4	Fe, N	Pyrolysis process followed by the post-treatment with $FeSO_4$ (used as precursor of Fe)	Aromatic N-C=N covalent bonds, Fe-N coordination bonds	XPS FT-IR spectra	Improved photocatalytic degradation of Rhodamine B (up to 98% within 60 min)	[131]
Pd/N-doped carbon catalyst	Pd, N	Carbonization of ionic liquids followed by wet-impregnation process	C-N covalent bonds (pyridinic, pyrrolic and graphitic-N), Pd-N and Pd-Cl coordination bonds	XPS XAS XRD analysis	Catalyst in acetylene hydrochlorination	[115]
Ni/Fe SA co-anchored trimodal porous carbon	Ni, Fe, N	Combined template, wetness-impregnation and pyrolysis method	Fe-N_x and Ni-N_x coordination bonds, C-N covalent bonds (pyridinic and graphitic-N)	XPS N K-edge XANES spectrum EXAFS spectrum	Enhanced ORR catalytic activity due to the Ni-N_4/Fe-N4 coordination bonds	[170]

Rare earth (Y/Sc) SA doped carbons	N, Y, Sc	One step solid synthesis method	M-N_x coordination bond	XAS XANES spectrum EXAFS spectrum DFT calculations	Improved CO_2RR catalytic activity	[171]
Fe-N doped carbons	Fe, N	Plasma enhanced chemical vapour deposition	Fe-N coordination bonds	XPS Micro-Raman Spectroscopy	Improved ORR activity, possible application in fuel cells	[172]
Co SA embedded N-doped carbon nanosheets	Co, N	Pyrolysis process	O=Co=O, C-N covalent bonds (pyrrolic and pyridinic-N), Co-N_4 coordination bonds.	XPS XAFS spectrum	Catalysis in the oxidation of benzene to form phenol	[173]
S-doped carbon dots	S	Hydrothermal process	C-S, C-N, C=O covalent bonds	XPS	Instigation of cancer cell apoptosis (by acting as a PI_3K/Akt inhibitor)	[174]
S, N doped layered carbon composites	S, N	Hydrothermal-calcination method	C-S, C=S, C-O-C, C-N covalent bonds (graphitic, pyridinic and pyrrolic-N)	Raman Spectra XPS	Superior HER electrocatalytic activity, preparation of high energy storage anodes for supercapacitors.	[175]
S-doped porous hollow carbon spheres	S	Template based polymerization process	C-S covalent bonds	XPS	Preparation of various S-doped CBMs with tailored pore structure	[176]

EELS= electron energy loss spectroscopy, ICP-AES= inductively coupled plasma-atomic emission spectrometry, XAS= X-ray absorption spectra, XANES= X-ray absorption near edge structure, EXAFS= X-ray absorption fine structure, XAFS= element selective X-ray absorption fine structure, N/A= Not available.

6. Perspectives of Carbon Doping

Carbon can be doped in different ways in order to boost its performance for different applications. However, it is still challenging to synthesize a material with high loading of isolated metal atoms. Perhaps, the most noticeable advances in this process is to discover the atomically dispersed single atom based supporting materials for various advance applications. This is due to the fact that when metal nanoparticles are downsized to single atoms, the traditional metal-semiconductor junction, where a Schottky barrier exists, would disappear. Anyway, to understand the fundamental doping strateiges, different general chemistries are adoped and hypothized as discussed in previous sections. Aprat from them, there are some rooms to consider for further improvement in carbon doping. They are listed in below:

i. A thorough grasp of the many types and structures of active sites should be developed in order to get the similar values via experimental techniques which is predicted via theortical dopant concentration. Although some techniques have been already applied, there is still plenty of room for improvement in this area. For instance, ORR activity is often higher when many heteroatoms are doped into carbon materials than when only a single heteroatom is doped. On the other hand, the synergetic process remains unknown, which might open up many possibilities for developing new, more efficient catalysts.

ii. The pore structure, specific surface area, and electrical conductivity of electrocatalysts must all be optimized coherently in order to improve the overall catalytic efficiencies. For instance, the precise link between pore size and mass transport capabilities of mesopores and macropores to active substance exchange in various mediums is yet to be understood.

iii. The development of active sites is the fundamental requisition of catalyst design. But a catalyst's performance to date is still poor, and more efficient ways must be devised[177]. Thus, the effects of the interaction between single metal atoms and supports on the charge separation and transfer processes must be studied in depth.

iv. Although, there are losts of computional approaches have been put forwared to understand the structure-activity relationship and also the orientations of the atoms in the core carbon structure, in-depth analyses of the computational simulated results and the development of more sophisticated computational tools that are capable of accurately measuring the change during doping sepecially while atomic level is controlled are still needed. To do this, the atomic configuration and rearrangement during the doping should be clearly visualized in terms of molecular orientation, spin-density redistribution, orbital position changing and so on.

v. It would be helpful for understanding the doping chemistries of CBMs if the dynamic reaction process or preparation process of dopants in CBMs can be visualized or monitored during experiment via different new techniques, to unlock the full mechanism.

vi. There are lots of attemptes being put forwared on 3D/4D printing of different meterails. However, no significant improvement on the atomic level control has been achieved. The fine tune of real molecular mixing and the controlling the preparation processes into printing formate could eventually help to understand the natural forming the materials.

vii. Most of the applications of doped CBMs are mainly focus on catalysis areas and some electronic applications. However, these applications need to extend into versatile routes to identify the potential of doped-carbons.

7. Conclusion

The fundamental chemistry of CBMs doping with different atoms, the underlying mechanisms, and the effect of doping on various chemical states of CBMs have been discussed. Atoms can be doped in CBMs in two ways either by C-atom substitution or through intercalation in the carbon lattice. The in-situ doping of CBMs is appropriate for achieving homogenous structure with

doped elements, while post-doping of CBMs leads to a change in surface functionalization without altering CBMs' bulk properties. Doping with single heteroatoms (e.g., N, B, O, S, X, M, and so on) is mainly carried out for electrical modulation, whereas co-doping with different foreign atoms promotes charge transfer efficiency, introduces asymmetric spin density and alike. In most cases, covalent and coordination bonds are formed between the dopants and carbon atoms of the lattice.

The main considerations of doping include Fermi-level-induced compensation effects, chemical potentials of the different elements, and local bonding effects of the dopant to the lattice. The foreign atoms whose electron affinity and electronegativity are different from those of the carbon atoms result in redistribution of the configuration of the electrons and their spin density, leading to higher charge delocalization, band gap opening (or widening) and change of hybridization when introduced in the CBMs. However, some future focus should give on the rational engineering design, molecular level control and developing proper computational simulations to understand the fundamentals of CBMs.

8. Reference

1. Burchell, T. D., *Carbon materials for advanced technologies*. Elsevier: 1999
2. Dai, L.*, et al.*, *Chemical Reviews* (2015) **115** (11), 4823
3. Avouris, P.*, et al.*, Carbon-based electronics. In *Nanoscience And Technology: A Collection of Reviews from Nature Journals*, World Scientific(2010), pp 174
4. Erwin, S. C.*, et al.*, *Nature* (2005) **436** (7047), 91
5. Luo, Z.*, et al.*, *Applied Physics Letters* (2012) **100** (25), 253108
6. Higgins, D.*, et al.*, *Energy & Environmental Science* (2016) **9** (2), 357
7. Zhou, M.*, et al.*, *Chemical Society Reviews* (2016) **45** (5), 1273
8. Tao, L.*, et al.*, *Advanced Energy Materials* (2019), 1901227
9. Guo, D.*, et al.*, *Science* (2016) **351** (6271), 361
10. Inagaki, M.*, et al.*, *Carbon* (2018) **132**, 104
11. Deng, Y.*, et al.*, *Journal of Materials Chemistry A* (2016) **4** (4), 1144
12. Agnoli, S., and Favaro, M., *Journal of Materials Chemistry A* (2016) **4** (14), 5002

13. Nistor, R. A.*, et al.*, *ACS nano* (2011) **5** (4), 3096
14. Duclaux, L., *Carbon* (2002) **40** (10), 1751
15. Ayala, P.*, et al.*, *Carbon* (2010) **48** (3), 575
16. Zunger, A., *Applied Physics Letters* (2003) **83** (1), 57
17. Cui, H.*, et al.*, *Materials Horizons* (2017) **4** (1), 7
18. Gao, K.*, et al.*, *Advanced Materials* (2019) **31** (13), 1805121
19. Zheng, Y.*, et al.*, *Angewandte Chemie International Edition* (2013) **52** (11), 3110
20. Sun, C.-L.*, et al.*, *Journal of the American Chemical Society* (2006) **128** (26), 8368
21. Guo, B.*, et al.*, *Nano letters* (2010) **10** (12), 4975
22. Lin, Y.-C.*, et al.*, *Applied Physics Letters* (2010) **96** (13), 133110
23. Brenner, K., and Murali, R., *Applied Physics Letters* (2010) **96** (6), 063104
24. Jiang, H. R.*, et al.*, *The Journal of Physical Chemistry C* (2016) **120** (12), 6612
25. Tsang, J.*, et al.*, *Nature nanotechnology* (2007) **2** (11), 725
26. Nevidomskyy, A. H.*, et al.*, *Physical review letters* (2003) **91** (10), 105502
27. Glerup, M.*, et al.*, *Chemical Communications* (2003) (20), 2542
28. Baei, M. T.*, et al.*, *Physics Letters A* (2012) **377** (1-2), 107
29. Curran, S. A.*, et al.*, *Journal of Applied Physics* (2009) **105** (7), 073711
30. Silva, L. A.*, et al.*, *IEEE transactions on nanotechnology* (2006) **5** (5), 517
31. Henkelman, G.*, et al.*, *Computational Materials Science* (2006) **36** (3), 354
32. Talla, J. A., *Physica B: Condensed Matter* (2012) **407** (6), 966
33. Peng, S., and Cho, K., *Nano letters* (2003) **3** (4), 513
34. Liang, J.*, et al.*, *Angewandte Chemie International Edition* (2012) **51** (46), 11496
35. Hu, C., and Dai, L., *Advanced Materials* (2017) **29** (9), 1604942
36. Song, Y.*, et al.*, *RSC Advances* (2016) **6** (97), 94636
37. Lin, H.*, et al.*, *New Journal of Chemistry* (2016) **40** (7), 6022
38. Chen, K.*, et al.*, *RSC Advances* (2017) **7** (10), 5782
39. Yang, S.*, et al.*, *Angewandte Chemie International Edition* (2016) **55** (12), 4016
40. Yue, X.*, et al.*, *Journal of Materials Chemistry A* (2017) **5** (17), 7784

41. Fu, Y. a., *et al.*, *European Journal of Inorganic Chemistry* (2016) **2016** (13-14), 2100
42. Qu, K., *et al.*, *ACS nano* (2017) **11** (7), 7293
43. Sun, T., *et al.*, *Chemistry–A European Journal* (2016) **22** (30), 10326
44. Zhang, J., *et al.*, *Angewandte Chemie International Edition* (2016) **55** (6), 2230
45. Zheng, Y., *et al.*, *ACS nano* (2014) **8** (5), 5290
46. Chen, Y., *et al.*, *Joule* (2018) **2** (7), 1242
47. Han, A., *et al.*, *Small Methods* (2019), 1800471
48. Fei, H., *et al.*, *Chemical Society Reviews* (2019)
49. Moisala, A., *et al.*, *Journal of Physics: condensed matter* (2003) **15** (42), S3011
50. Lee, B.-H., *et al.*, *Nature materials* (2019) **18** (6), 620
51. Yang, X.-F., *et al.*, *Accounts of chemical research* (2013) **46** (8), 1740
52. Qiao, B., *et al.*, *Nature chemistry* (2011) **3** (8), 634
53. Han, B., *et al.*, *Chinese Journal of Catalysis* (2017) **38** (9), 1498
54. Maschmeyer, T., *et al.*, *Nature* (1995) **378** (6553), 159
55. Liu, P., *et al.*, *Science* (2016) **352** (6287), 797
56. Hossain, M. D., *et al.*, *Advanced Energy Materials* (2019) **9** (10), 1803689
57. Zhang, Y., *et al.*, *Small Methods* (2019) **3** (9), 1800406
58. Wang, B., *et al.*, *Small Methods* (2019), 1800447
59. Sachs, B., *et al.*, *Applied Physics Letters* (2013) **103** (25), 251607
60. Zhang, J., *et al.*, *Small Methods* (2019), 1800481
61. Giovannetti, G., *et al.*, *Physical review letters* (2008) **101** (2), 026803
62. Khomyakov, P., *et al.*, *Physical Review B* (2009) **79** (19), 195425
63. Payne, M. C., *et al.*, *Reviews of modern physics* (1992) **64** (4), 1045
64. Kresse, G., and Furthmüller, J., *Computational materials science* (1996) **6** (1), 15
65. Zhou, X., *et al.*, *Applied Surface Science* (2018) **459**, 354
66. Perdew, J. P., *et al.*, *Physical review letters* (1996) **77** (18), 3865
67. Tang, Y., *et al.*, *The Journal of Physical Chemistry C* (2013) **117** (10), 5258
68. Zhuo, H.-Y., *et al.*, *Chemical reviews* (2020) **120** (21), 12315

69. Zhang, Q.*, et al.*, *Nanotechnology* (2020) **32** (3), 032001
70. Giovannetti, G.*, et al.*, *Physical review letters* (2008) **101** (2), 026803
71. Yin, J.*, et al.*, *Journal of the American Chemical Society* (2016) **138** (44), 14546
72. Baglio, V.*, et al.*, *Journal of the Electrochemical Society* (2008) **155** (8), B829
73. Guo, S.*, et al.*, *Angewandte chemie international edition* (2012) **51** (47), 11770
74. Guo, S., and Sun, S., *Journal of the American Chemical Society* (2012) **134** (5), 2492
75. Yu, Z.*, et al.*, *Small* (2020) **16** (23), 1907233
76. Wang, Q.*, et al.*, *Applied Surface Science* (2017) **397**, 199
77. Guo, B.*, et al.*, *Insciences J.* (2011) **1** (2), 80
78. Fei, H.*, et al.*, *Nature Catalysis* (2018) **1** (1), 63
79. Kwon, H. C.*, et al.*, *Journal of the American Chemical Society* (2018) **140** (47), 16198
80. Dai, L., *Accounts of chemical research* (2012) **46** (1), 31
81. Zhao, L.*, et al.*, *Science* (2011) **333** (6045), 999
82. Cruz-Silva, E.*, et al.*, *ACS Nano* (2009) **3** (7), 1913
83. Terrones, M., *Annu. Rev. Mater.Res* (2003) **13**, 419
84. Terrones, M.*, et al.*, *Materials Today* (2004) **7** (10), 30
85. Guo, B.*, et al.*, *Insciences Journal* (2011) **1**, 80
86. Rani, P., and Jindal, V., *RSC Advances* (2012) **3**, 802
87. Castro Neto, A. H.*, et al.*, *Reviews of Modern Physics* (2009) **81** (1), 109
88. Panchakarla, L. S.*, et al.*, *Advanced Materials* (2009) **21** (46), 4726
89. Zhang, Y.-F.*, et al.*, *Nano Research* (2017) **10** (10), 3377
90. Houmad, M.*, et al.*, *Carbon* (2015) **94**, 1021
91. Choi, C. h.*, et al.*, *Journal of Materials Chemistry A* (2013) **1**, 3694
92. Ma, R.*, et al.*, *npj Computational Materials* (2019) **5** (1), 78
93. Koretsune, T., and Saito, S., *Physical Review B* (2008) **77** (16), 165417
94. Lee, W. J.*, et al.*, *Chemical Communications* (2014) **50** (52), 6818
95. Geim, A. K., and Novoselov, K. S., *Nature Materials* (2007) **6** (3), 183
96. Zhang, C.*, et al.*, *Advanced Materials* (2011) **23** (8), 1020

97. Kaloni, T. P.*, et al.*, *Applied Physics Letters* (2014) **104** (7), 073116

98. Zhang, J.*, et al.*, *Nature Nanotechnology* (2015) **10** (5), 444

99. Yang, N.*, et al.*, *Chemical Science* (2018) **9** (26), 5795

100. Jin, Z.*, et al.*, *Nanoscale* (2012) **4** (20), 6455

101. Zhang, L.*, et al.*, *The Journal of Physical Chemistry C* (2014) **118** (7), 3545

102. Zhang, L., and Xia, Z., *The Journal of Physical Chemistry C* (2011) **115** (22), 11170

103. Qu, K.*, et al.*, (2017) **7** (9), 1602068

104. Ishii, S., and Takano, Y., *Spie Newsroom* (2007)

105. Podyacheva, O. Y.*, et al.*, *Carbon* (2017) **122**, 475

106. Alarifi, I. M., *Journal of Materials Research and Technology* (2019) **8** (5), 4863

107. Wilder, J. W. G.*, et al.*, *Nature* (1998) **391** (6662), 59

108. Yu, X., and Manthiram, A., *Applied Catalysis B: Environmental* (2015) **165**, 63

109. Liu, M.*, et al.*, *Chemical Reviews* (2014) **114** (10), 5117

110. Cong, K.*, et al.*, *Electroanalysis* (2014) **26** (12), 2567

111. Ekimov, E. A.*, et al.*, *Nature* (2004) **428** (6982), 542

112. Chen, T.*, et al.*, *Dalton Transactions* (2014) **43** (40), 14931

113. Hoang, V. C.*, et al.*, *Carbon* (2020) **157**, 515

114. Ismagilov, Z. R.*, et al.*, *Carbon* (2009) **47** (8), 1922

115. Zhang, Z. J.*, et al.*, *Ionics* (2020) **26** (6), 3027

116. Fujisawa, K.*, et al.*, *Nanoscale* (2011) **3** (10), 4359

117. Ibrahim, E. M. M.*, et al.*, *Diamond and Related Materials* (2010) **19** (10), 1199

118. Chen, H.*, et al.*, *The Journal of Physical Chemistry C* (2013) **117** (16), 8318

119. Wiggins-Camacho, J. D., and Stevenson, K. J., *The Journal of Physical Chemistry C* (2009) **113** (44), 19082

120. Ishii, S., and Takano, Y., High-conductivity boron-doped carbon nanotubes. Citeseer

121. Schiros, T.*, et al.*, *Nano Letters* (2012) **12** (8), 4025

122. Salzmann, I.*, et al.*, *Physical Review Letters* (2012) **108** (3), 035502

123. Latha, B.*, et al.*, *Journal of Molecular Structure* (2018) **1152**, 351

124. Kim, H.*, et al.*, *Physical Chemistry Chemical Physics* (2011) **13** (39), 17505
125. Yadav, A.*, et al.*, *The Journal of Physical Chemistry C* (2017) **121** (31), 16721
126. Mahamiya, V.*, et al.*, *Journal of Alloys and Compounds* (2022) **897**, 162797
127. Gangan, A.*, et al.*, *International Journal of Hydrogen Energy* (2019) **44** (31), 16735
128. Chakraborty, B.*, et al.*, *International Journal of Hydrogen Energy* (2021) **46** (5), 4154
129. Bulushev, D. A.*, et al.*, *Acs Catalysis* (2016) **6** (6), 3442
130. Chen, X.*, et al.*, *Applied Surface Science* (2020) **526**, 146626
131. Duan, L.*, et al.*, *Optical Materials* (2021) **118**, 111222
132. Paraknowitsch, J. P.*, et al.*, *Journal of Materials Chemistry* (2010) **20** (32), 6746
133. Pietrzak, R.*, et al.*, *Energy & fuels* (2006) **20** (3), 1275
134. Burg, P.*, et al.*, *Carbon* (2002) **40** (9), 1521
135. Li, Y.*, et al.*, *Journal of the American Chemical Society* (2012) **134** (1), 15
136. Pang, Y.*, et al.*, *Materials Letters* (2017) **193**, 236
137. Hu, Y.*, et al.*, *Applied Surface Science* (2020) **531**, 147344
138. Guldi, D. M.*, et al.*, *Chemical Society Reviews* (2006) **35** (5), 471
139. Axet, M. R.*, et al.*, *Coordination Chemistry Reviews* (2016) **308**, 236
140. Yan, Q.-Q.*, et al.*, *Nature communications* (2019) **10** (1), 1
141. Cao, L.*, et al.*, *Nature Catalysis* (2019) **2** (2), 134
142. Fei, H.*, et al.*, *Nature communications* (2015) **6** (1), 1
143. Sa, Y. J.*, et al.*, *ACS Catalysis* (2018) **9** (1), 83
144. Lu, B.*, et al.*, *Nature communications* (2019) **10** (1), 1
145. Liu, D.*, et al.*, *Nature Energy* (2019) **4** (6), 512
146. Lee, Y.-S., *Journal of Fluorine Chemistry* (2007) **128** (4), 392
147. Kim, J.*, et al.*, *RSC advances* (2018) **8** (26), 14152
148. Zhao, Z., and Xia, Z., *Acs Catalysis* (2016) **6** (3), 1553
149. Di Vittorio, S.*, et al.*, *Journal of materials research* (1993) **8** (7), 1578
150. Nakajima, T.*, et al.*, *Electrochimica acta* (2000) **45** (10), 1655
151. Mingyi, L.*, et al.*, *Journal of Power Sources* (2008) **177** (2), 493

152. Satyapal, S.*, et al.*, *Catalysis today* (2007) **120** (3-4), 246
153. (!!! INVALID CITATION !!! [173-175])
154. Liu, C.*, et al.*, *Science* (1999) **286** (5442), 1127
155. (!!! INVALID CITATION !!! [176-178])
156. Prakash, M.*, et al.*, *International journal of hydrogen energy* (2011) **36** (6), 3922
157. (!!! INVALID CITATION !!! [179-181])
158. Sun, Q.*, et al.*, *Journal of the American Chemical Society* (2006) **128** (30), 9741
159. Schnorr, J. M., and Swager, T. M., *Chemistry of Materials* (2011) **23** (3), 646
160. Chandrakumar, K., and Ghosh, S. K., *Nano letters* (2008) **8** (1), 13
161. Xie, J.*, et al.*, *Angewandte Chemie* (2019) **131** (15), 5017
162. Ji, Q.*, et al.*, *Chemical Engineering Journal* (2018) **350**, 608
163. Zhou, M.*, et al.*, *Applied Catalysis B: Environmental* (2020) **273**, 119007
164. Robertson, J., and Davis, C., *Diamond and Related Materials* (1995) **4** (4), 441
165. Ticknor, B.*, et al.*, *The Journal of Physical Chemistry A* (2008) **112** (48), 12355
166. Peng, P.*, et al.*, *ACS nano* (2019) **13** (1), 878
167. Wang, C.*, et al.*, *Materials Chemistry and Physics* (2019) **232**, 145
168. Gao, J.*, et al.*, *Catalysis Science & Technology* (2018) **8** (4), 1142
169. Liu, Q.*, et al.*, *ACS Applied Materials & Interfaces* (2020) **12** (15), 17641
170. Zhu, Z.*, et al.*, *Advanced Materials* (2020) **32** (42), 2004670
171. Liu, J.*, et al.*, *ACS nano* (2020) **14** (1), 1093
172. Hotozuka, K.*, et al.*, *Chemical Physics Letters* (2017) **679**, 71
173. Zhu, Y.*, et al.*, *Nature communications* (2018) **9** (1), 1
174. Li, Y.*, et al.*, *Cell proliferation* (2020) **53** (5), e12821
175. Atchudan, R.*, et al.*, *Journal of Electroanalytical Chemistry* (2019) **833**, 357
176. Böttger-Hiller, F.*, et al.*, *Chemical Communications* (2012) **48** (85), 10568
177. Li, J. C.*, et al.*, *Small* (2017) **13** (45), 1702002